Title
Imaging evaluation of osteomyelitis.

Journal
Journal of Cardiovascular Magnetic Resonance, 35(3)

ISSN
1548-7679

Authors
Crim, JR
Seeger, LL

Publication Date
1994

Peer reviewed

Critical Reviews in Diagnostic Imaging, 35(3):201–256 (1994)

Imaging Evaluation of Osteomyelitis

Julia R. Crim, M.D.[1] and Leanne L. Seeger, M.D.[2]

[1]Durham Radiology Associates, 2609 N. Roxboro Street, Durham, North Carolina 27704, [2]Department of Radiological Sciences, Musculoskeletal Radiology, UCLA School of Medicine, 200 UCLA Medical Plaza, Suite 165-59, Los Angeles, California 90024-6952

ABSTRACT: Bone infection, or osteomyelitis, is a common medical problem that is often difficult to diagnose. Osteomyelitis is not unusual in diabetic patients with foot ulcers and bedridden patients with decubitus ulcers — populations where diagnosis is especially difficult. Spinal osteomyelitis and septic arthritis require early diagnosis in order to avoid permanent debilitating consequences. Regardless of the clinical setting, imaging plays an important role in establishing the diagnosis and directing treatment. A variety of imaging modalities may be used, including plain radiography, radionuclide imaging, computed tomography (CT), and magnetic resonance imaging (MRI). Decisions regarding the best imaging modality can be challenging and should reflect the location of the suspected infection and associated illness or bony disorders.

KEY WORDS: bone infection, osteomyelitis, imaging.

I. INTRODUCTION*

Osteomyelitis is a serious medical problem that is associated with significant patient morbidity and substantial financial burden. Parenteral antibiotics are required for treatment, and patients requiring repeated surgical debridement are often subjected to prolonged hospitalization. Accurate, early diagnosis necessary to optimize treatment strategies often requires investigation with imaging. The choice of imaging techniques employed will depend on the patient population, the location of the infection, and the presence of underlying bone abnormalities. Imaging spine infection, for example, may differ from imaging infection in the extremities. Similarly, imaging suspected osteomyelitis with overlying soft-tissue abnormality may differ from imaging chronic osteomyelitis related to fracture nonunion or orthopedic hardware.

The following discussion outlines imaging modalities utilized to diagnose osteomyelitis. The various types of osteomyelitis are reviewed, emphasizing the optimal methods for diagnosis in each group.

* All figures for this article appear following the text and before the list of references.

1040-8371/94/$.50

II. PATHOGENESIS

Osteomyelitis may result from hematogenous seeding, spread from adjacent soft-tissue infection, or direct inoculation. Hematogenous spread is most common in children. Osteomyelitis due to adjacent soft-tissue infection is commonly associated with neurotrophic foot ulcers in diabetic patients and decubitus ulcers in bedridden patients. Direct inoculation may occur in the setting of trauma (puncture wound or open fracture) or surgery.

Bacterial infection of bone requires vascular stasis to promote localization of the bacteria, and a suitable environment for growth such as blood clot, plasma, or necrotic tissue.[1] In children, these conditions are met in the metaphyses of long bones where capillaries drain into large veins in which blood flow is slow.[2,3] Childhood osteomyelitis is most common in the tibia and femur, a predilection that may be related to the frequency of knee trauma and subsequent occult metaphyseal bleeding.[1] In the adult, metaphyseal blood stasis does not usually occur, and osteomyelitis of the metaphysis of long bones is uncommon except following fracture. Instead, hematogenous osteomyelitis in the adult occurs most commonly in the vertebrae or the subchondral portion of long bones where slow flow is seen.

In the infant, blood vessels cross the physis. Thus, infection may be hematogenously spread from the metaphysis into the epiphysis. After the age of 1 year, metaphyseal capillaries make hairpin turns back on themselves at the physeal plate rather than crossing it. Spread of infection into the epiphysis in the older child or adult is therefore unusual.

III. RADIOLOGIC METHODS OF DIAGNOSIS

A. Plain Radiographs

Bony abnormalities related to osteomyelitis are generally not evident on plain radiographs until 10 to 20 d after the onset of symptoms.[4,5] In an experimental animal model, Raptopoulos[6] found bone radiographs to be abnormal on day 12 after injection of *Staphylococcus*. Muscle swelling and subtle loss of soft-tissue plane definition may be seen earlier, especially in children[4,6] (Figure 1A). However, despite this delay between inoculation and radiographic alteration, plain radiographs should always be the initial imaging undertaken for suspected osteomyelitis.

The radiographic appearance of acute osteomyelitis is identical to that seen in other round cell lesions of bone, including Ewing's sarcoma, Langerhan's cell histiocytosis (formerly known as histiocytosis X), and lymphoma. Metastasis, myeloma, lytic osteosarcoma, fibrosarcoma, and malignant fibrous histiocytoma can also have this appearance. Although plain film findings are not pathognomonic for infection, a definitive diagnosis may often be made when radiographic changes

are combined with information obtained from clinical history, physical examination, and laboratory findings. In the appropriate setting, additional imaging may not be needed.

Acute osteomyelitis has a permeative pattern on plain radiographs. Characteristic findings include osteopenia with small, ill-defined lucencies in the medullary bone and cortex. Cortical destruction may be evident (Figure 2). The zone of transition to normal bone is wide. Periostitis is common in children, but it is seen less often in adults.[7] When orthopedic hardware is present, osteomyelitis appears as a poorly marginated lucency surrounding the device (Figure 3). Differentiation between infection and aseptic hardware loosening may be difficult, but the distinction can often be made by evaluating the shape of the lucency. When the bone lysis is a round focus, infection is likely. Aseptic loosening of hardware will usually have a more cone-shaped configuration that tapers gradually from the point of maximum motion of the metal to the point where motion is least.

Advanced cases of ósteomyelitis may show sequestration of dead, sclerotic bone. In children, exuberant periosteal reparative bone (the involucrum) may surround the sequestrum (Figure 1B). A cloaca (Latin for sewer) is a sinus tract that extends from the medullary cavity to the surface of the bone. Although diagnostic of longstanding osteomyelitis, these signs are now less commonly seen than in the pre-antibiotic era.

The Brodie's abscess represents subacute osteomyelitis. The distinctive radiographic appearance of this entity is discussed below.

B. Technetium

When plain radiographs are normal or equivocal and osteomyelitis is suspected, the three phase technetium radionuclide bone scan is often useful in differentiating between cellulitis and osteomyelitis. Scans are performed during and immediately following the intravenous administration of 10 to 20 mCi of technetium 99m-labeled diphosphonate, generally methylene diphosphonate (^{99m}Tc-MDP), and 2 to 4 h following injection. The diphosphonate will initially distribute throughout the body in an amount proportional to blood flow. As the tracer is cleared by the kidneys, soft-tissue accumulation of tracer declines. Diphosphonates are initially taken up by bone by chemisorption and are later incorporated into bone matrix and crystal in an amount proportional to osteoblastic activity.[8] Thus, bone uptake increases over time as soft-tissue accumulation declines. In the patient with normal renal function, soft-tissue uptake will be minimal compared with bone uptake in 2 to 4 h. In the setting of cellulitis without osteomyelitis, tracer activity will be increased in early images, but normal on delayed images. Noninflammatory bone conditions such as ischemic necrosis, degenerative arthritis, and many bone tumors demonstrate normal activity on early images and increased activity on delayed images.[9] Osteomyelitis results in both increased blood flow and increased

osteoblastic activity,[9] thus increased tracer accumulation will be evident in both early and delayed images.

The first phase of the three-phase radionuclide scan is the radionuclide angiogram, during which images are obtained every 4 to 5 s. Osteomyelitis will generally show increased arterial flow in the early angiogram phase. Increased activity in the venous portion of the radionuclide may be due to cellulitis.[10] The second phase of the three-phase bone scan, the blood pool image, is obtained immediately following the angiogram. Increased soft-tissue activity in the blood pool phase is due to hyperemia and may be seen with either cellulitis or osteomyelitis. The third phase of the scan is obtained 2 to 4 h after radionuclide injection. These static images reflect bone uptake of radionuclide due to osteoblastic activity. In equivocal cases, a fourth phase may be obtained at 24 h when the ratio of bone to soft-tissue uptake is higher.[11,12] Cellulitis is expected to demonstrate decreasing uptake, and osteomyelitis will demonstrate increasing uptake that is localizable to the bone (Figure 4).

The accuracy of the three-phase bone scan varies according to the clinical setting. In a diverse population without other underlying bone abnormalities, sensitivity and specificity as high as 92 and 96%, respectively, have been reported.[9] Sensitivity is lower in young children and has been reported as low as 32% in neonates.[13] Specificity is lower in the diabetic population and patients in whom other bone abnormalities are present. Although there are numerous causes of positive three-phase bone scans (Table 1), many of these conditions can be differentiated from osteomyelitis on plain radiographs.

Although the three-phase bone scan is useful in diagnosing established osteomyelitis, the study may be normal in the early stages of infection. One animal study[14] found that only 22% of cases of osteomyelitis showed a diagnostic three-phase bone scan during the first week following injection of *Staphylococcus aureus*. During this same early stage of infection, 83% of Indium-111 white blood cells (^{111}In WBC) scans and 67% of CT scans were abnormal.

TABLE 1
Causes of Positive Three-Phase Bone Scan

Osteomyelitis
Neuropathic (Charcot) joint
Cellulitis
Acute fracture
Fracture nonunion
Recent surgery
Vascular tumor (some sarcomas and metastases, osteoid osteoma, hemangioma)
Reflex sympathetic dystrophy
Inflammatory arthritis (e.g., gout, rheumatoid arthritis)
Aseptic loosening of joint replacement or other orthopedic hardware

C. Gallium

Correlating the ^{99m}Tc-MDP bone scan with Gallium-67 citrate (^{67}Ga) scans has been advocated to increase the specificity of the ^{99m}Tc-MDP scan.[15–17] ^{67}Ga localizes at sites of inflammation. It has a half-life of 78 h and is excreted by the kidneys, the biliary system, and the bowel. For imaging, 4 to 6 mCi of ^{67}Ga are injected intravenously. Scanning is performed at 4 to 6 h and repeated at 24-h intervals as needed. The ^{67}Ga scan is considered positive for osteomyelitis if the degree of tracer uptake is greater than the ^{99m}Tc-MDP uptake in the same area.

Unfortunately, the specificity of ^{67}Ga for infection is low. Schauwecker and colleagues studied ^{99m}Tc-MDP, ^{67}Ga, and ^{111}In WBC scans for osteomyelitis in 57 patients.[16] All but nine had an underlying condition that could cause false-positive three-phase bone scan, including prior bone surgery, prosthesis, fracture, neuropathic osteopathy, and arthritis. They found that sensitivity of ^{67}Ga was 100%, but specificity was only 25%; ^{67}Ga scan added information beyond that obtained on ^{99m}Tc-MDP bone scans in only 28% of patients. ^{67}Ga accumulation thus nonspecifically reflects infection, aseptic inflammation, and trauma. Increased ^{67}Ga localization may also be seen in certain tumors.

Recently, Sorsdahl and colleagues[18] examined 110 patients with suspected osteomyelitis with quantitative analysis of ^{67}Ga uptake compared with ^{99m}Tc-MDP uptake. Osteomyelitis was diagnosed if two of the following three criteria were met: ^{67}Ga/^{99m}Tc-MDP ratio greater than or equal to 0.7, ^{67}Ga/background ratio greater than or equal to 2.0, and spatial incongruence of ^{67}Ga and ^{99m}Tc-MDP activity. Using these criteria, they found a 70% sensitivity and 93% specificity.

D. Indium

^{111}In WBC scans have been used extensively to aid in the diagnosis of infection. Scans are performed using 0.5 to 1.0 mCi of ^{111}In, and imaging is performed 18 to 24 h following injection. ^{111}In has a half-life of 67 h. The labeled white cells are sequestered in the spleen, liver, bone marrow, and any site where there are increased numbers of white blood cells.

^{111}In WBC scanning has been reported to be positive at an earlier stage of osteomyelitis than the ^{99m}Tc-MDP bone scan.[14] In patients with underlying bone conditions, Schauwecker[16] found that ^{111}In WBC scans had a sensitivity of 100% for acute osteomyelitis and 60% for chronic osteomyelitis, with a specificity of 96%. Antibiotic therapy does not affect the sensitivity of ^{111}In WBC scans.[19] ^{111}In WBC scanning is more accurate in the extremities than in the axial skeleton where erythropoietic marrow is present.[20] Although ^{111}In WBC scanning may detect osteomyelitis at an earlier stage than ^{99m}Tc-MDP, the spatial resolution of ^{111}In

WBC scans is poor, and it may be difficult to determine if activity is in bone or soft tissue (Figure 4D).

False-positive ^{111}In WBC scans may be encountered in cases of fracture.[21] Accuracy is increased when concomitant ^{99m}Tc-MDP bone scanning is performed and the location of ^{111}In WBC activity is compared with that of ^{99m}Tc-MDP.[20] The sensitivity, specificity, and accuracy of ^{111}In WBC scans can also be increased by combining the ^{111}In WBC scan with ^{99m}Tc-sulfur colloid (SC) imaging. Incongruent uptake (labeled leukocyte activity without corresponding sulfur colloid activity) has been shown to be associated with 100% sensitivity and 97% specificity when evaluating total hip arthroplasty.[22]

^{111}In WBC may be used to label immunoglobulin.[21] Fischman and colleagues[23] found that indium-labeled IgG was true positive in eight cases of osteomyelitis and true negative in seven cases of suspected osteomyelitis. There were no false-positive or false-negative scans. Indium-labeled IgG will, however, also accumulate in noninfectious inflammatory processes.[23]

E. Technetium-HMPAO

Technetium hexamethylpropyleneamine oxide (^{99m}Tc-HMPAO) labeled white cells have been advocated as a less-expensive and lower radiation alternative to ^{111}In. Lantto and colleagues[24] found a sensitivity in abdominal infections of 95% and a specificity of 85%. Although an attractive alternative, labeling with technetium is time consuming, and the concentration of ^{99m}Tc-HMPAO in infection is less than that of ^{111}In WBC.[25]

F. Computed Tomography (CT)

Although cross-sectional imaging of osteomyelitis is now often accomplished with MRI, CT continues to play an important role. This is especially true in the patient with additional underlying bone abnormality such as fracture nonunion or infarction. One study subjectively found MRI to show infection more clearly than CT in 12 patients,[26] but no large study comparing the accuracy of CT to MRI has been published. CT demonstrates increased density of bone marrow in cases of osteomyelitis, a reflection of pus replacing normal fatty marrow. Foci of dense bone surrounded by fluid or soft-tissue density represent sequestra, and areas of cortical destruction are well seen.[27–31] Thus, CT is especially useful in planning surgical intervention,[31] including sequestrectomy and debridement. Intraosseous gas is more evident with CT than in plain radiographs and has been reported to be a sign of osteomyelitis.[30]

When searching for osteomyelitis, imaging without intravenous contrast is sufficient. Contrast enhancement will assist in defining soft-tissue abscesses and sinus tracts.

G. Magnetic Resonance Imaging (MRI)

In multiple studies, MRI has been found to have a very high sensitivity for detecting osteomyelitis (92 to 100%).[26,32–37] Because of this high sensitivity, many authors suggest that in the setting of normal or equivocal plain radiographs and a high clinical index of suspicion for osteomyelitis, MRI is the imaging modality of choice. Others, however, feel that the high cost of MRI renders it prohibitive to routinely use for the diagnosis of bone infection and favor the three-phase ^{99m}Tc-MDP bone scan as the next diagnostic intervention.

MRI evaluation of osteomyelitis generally employs T1- and T2-weighted images, often supplemented with short-tau-inversion-recovery (STIR) sequences. A focus of osteomyelitis will demonstrate low signal intensity on T1-weighted images and high signal intensity on T2-weighted and STIR sequences (Figure 5). Because STIR images produce high signal intensity for tissues with long T1 or long T2, they are more sensitive than spin echo images but less specific.

The specificity for MRI of osteomyelitis is lower than its sensitivity and has been reported to be as low as 82%.[37] Potential causes of false-positive scans include occult fracture,[30,32,34] infarction,[37] operative changes,[31] and neuropathic joints.[34,38] In addition, reactive marrow adjacent to foci of infection may show abnormal signal characteristics, and differentiation between infection and reactive inflammation is often not possible. Therefore, MRI may overestimate the extent of marrow abnormality.

Occult fractures can often be differentiated from osteomyelitis on MRI by identifying the fracture line within the area of abnormal marrow. Infarctions generally have a serpentine border that is not evident in acute osteomyelitis, but differentiation may be difficult (Figure 6). In the diabetic patient, differentiation of osteomyelitis and neuropathic joints may be problematic. This issue is discussed below.

IV. PEDAL OSTEOMYELITIS IN DIABETIC PATIENTS

Osteomyelitis of the foot is a common problem in diabetic patients and is often difficult to diagnose clinically. Fever and bacteremia are uncommon[39] and the erythrocyte sedimentation rate may be normal.

Ninety-four percent of cases of diabetic osteomyelitis in the foot are associated with ulcers.[39] Poor blood flow and insensitivity to pain lead to ulcer formation. The ulcers become infected, and the infection can spread to the underlying bone. Ulcers most commonly occur at pressure points on the foot, including the calcaneus, metatarsophalangeal joints, interphalangeal joints, and the tips of the toes. In one series,[39] 63% of cases of osteomyelitis involved the metatarsal heads, 57% were in the phalanges, and 8% involved the tarsal bones, usually the calcaneus. Necrotic debris in a neuropathic joint can also serve as an excellent nidus for infection.

Although it is generally accepted that osteomyelitis develops in about one third of deep ulcers that do not resolve with local care,[39] a recent study[40] suggests that osteomyelitis is much more common. Using bone biopsy and culture as a gold standard, osteomyelitis was found in 68% of 41 foot ulcers. Only 32% of cases had been diagnosed clinically. The majority of the cases of osteomyelitis occurred in outpatients with no evidence of inflammation on physical examination and were associated with ulcers that did not expose bone. If confirmed on further studies, these findings suggest that a more aggressive diagnostic approach to diabetic foot ulcers may be needed.

Percutaneous core bone biopsy can be used to diagnose osteomyelitis.[41,42] Biopsy makes organism-specific therapy possible, and a medical cure without amputation is more likely when specific antibiotics are given to eradicate an isolated pathogen.[40] Some authors favor open biopsy to the percutaneous approach, arguing that percutaneous biopsy may induce bone necrosis[39] or spread infection to noninfected bone. In addition, organisms in the ulcer may not be the same as those in the bone.[42,43] If performed, percutaneous biopsy should avoid the ulcer site.

The radiographic diagnosis of osteomyelitis in the diabetic population can be difficult. Table 2 summarizes the accuracy of the most commonly used imaging techniques. Plain radiographs have a lower sensitivity than other methods, but a specificity that is comparable to bone scan. False-positive radiographs are often associated with neuropathic joints or degenerative or inflammatory arthritis.[10] There are several plain radiographic findings that aid in the differentiation of infection from neuropathy. Neuropathic joints in the hindfoot and midfoot are hypertrophic with a large amount of reactive bone proliferation and debris (Figure 7). These findings are not seen in osteomyelitis, and thus differentiation is generally possible. In the forefoot, however, neuropathic joints are often atrophic and differentiation of the two entities is more difficult. The presence of osteoporosis and ill-defined erosions favor the diagnosis of osteomyelitis. Bone density is usually preserved in neuropathic joints.

Interpretation of the three-phase ^{99m}Tc-MDP bone scan is more problematic in diabetics than in the general population. This primarily reflects a high false-positive rate in the diabetic due to neuropathic (Charcot) joints or cellulitis. Reported mean sensitivity and specificity are 84% and 65%, respectively (Table 2), with the accuracy of the three-phase bone scan depending in part on the prevalence of neuropathic joint disease. Accuracy also depends on the site of the osteomyelitis; the specificity is lower in the hindfoot where neuropathic joints are common. One study[44] found a specificity of only 7% in the tarsometatarsal joints, an area where osteomyelitis is uncommon and neuropathic involvement is common. False-negative three-phase ^{99m}Tc-MDP bone scans may be seen in the diabetic patient due to a lack of blood flow to a region of osteomyelitis.[45]

TABLE 2
Accuracy of Imaging Techniques in Diabetic Pedal Osteomyelitis (Studies Are in Chronologic Order in Each Category)

Study	# pts	% sens[a]	% spec
Plain radiographs			
Park[44]	36	62	69
Seldin[10]	30	93	50
Larcos[45]	49	43	83
Newman[41]	41	28	92
Yuh[50]	29	75	75
Keenan[46]	88	69	82
Three-phase ^{99m}Tc-MDP bone scan			
Park[44]	36	83	75[a]
Seldin[10]	30	94	79
Larcos[45]	49	93	43
Israel[12]	38	82	92[b]
Maurer[47]	13	75	56
Yuh[50]	29	94	82
Keenan[46]	77	100	38
Newman[39]	41	69	39
Weinstein[43]	32	69	83
^{111}In WBC scan			
Larcos[45]	51	79	78
Schauwecker[48]	35	100	83[c]
Maurer[47]	13	75	89
Keenan[46]	46	100	78
Seabold[37]	16	80	69[c]
Newman[39]	41	89	89
MRI			
Yuh[50]	44	100	95
Wang[51]	46	99	81
Weinstein[43]	62	100	81

[a] Three patients with absent flow excluded from study; two of these had osteomyelitis.
[b] Quantitative four-phase bone scan.
[c] All patients had neuropathic foot disease with clinical question of superimposed osteomyelitis.

^{67}Ga scanning in the diabetic foot is generally not helpful because of the high number of false-positive scans. Although neuropathic joints can cause false-positive scans with all radionuclide modalities, ^{111}In WBC is the most specific for osteomyelitis and carries the highest sensitivity (Table 2). ^{111}In WBC scans can improve the specificity of the three-phase bone scan[38,40,46–49] but may be positive in as many as 31% of noninfected neuropathic joints.[38] False-positive scans are more likely to occur in rapidly progressive neuropathic joints than in neuropathic joints which are longstanding and radiographically stable.

Of available imaging modalities, MRI has the highest sensitivity for diagnosing osteomyelitis (Figure 5) and carries a high specificity for differentiating osteomyelitis from cellulitis in the diabetic (Figure 8). Thus, MRI is useful in evaluating suspected osteomyelitis in the setting of normal or nondiagnostic radiographs, or equivocal bone scans. Unger[50] found that five out of ten cases of cellulitis were misdiagnosed as osteomyelitis by ^{99m}Tc-MDP bone scan but were correctly diagnosed by MRI. He postulated that the false-positive bone scans were due to inflammation of the periosteum from overlying cellulitis and ulcers.

In evaluating osteomyelitis of the forefoot with MRI, scan planes must be carefully chosen to accurately image the small bones of the phalanges. This can be accomplished by using an axial localizer to align an oblique sagittal plane along the long axis of the abnormal ray and oblique coronal scans perpendicular to the ray. Routine T1- and T2-weighted spin echo imaging are generally sufficient, but STIR sequences will increase the conspicuity of marrow and soft-tissue abnormalities. Imaging may be performed in the head or extremity surface coil to cover relatively large areas or may be done with small surface coils to provide detailed resolution of a small area.

Figure 9 is a decision tree for imaging suspected osteomyelitis in the diabetic patient, which is based on both cost and accuracy of the different modalities. Plain radiographs should be obtained as the initial screening examination. If radiographic changes of osteomyelitis are present adjacent to an ulcer, treatment is indicated. If the radiograph is abnormal but an ulcer is absent, osteomyelitis is unlikely,[39] and the radiographic changes are more likely due to a resorptive neuropathic joint or arthritis. If the radiograph is normal and clinical suspicion is high, the low cost of the three-phase ^{99m}Tc-MDP bone scan may render it the next choice for diagnostic imaging. Although more expensive, MRI is an attractive alternative, and the choice of bone scan vs. MRI will reflect the local health-care environment. A positive bone scan or MRI with a normal radiograph is most likely due to osteomyelitis. If three-phase bone scan is negative, early osteomyelitis is not excluded.[14] The patient can either be followed with plain radiographs, or, if clinical suspicion is high, an MRI can be performed. MRI is also the procedure of choice when three-phase bone scan is equivocal, because it is better able than indium to accurately localize abnormalities to bone, periosteum, or soft tissue. If a neuropathic joint is evident radiographically, MRI is generally not indicated. Indium scanning can then be performed as an infection is unlikely in the face of a negative indium

study. Because indium can be falsely positive in neuropathic joints, a positive scan may be confirmed with biopsy.

V. OSTEOMYELITIS SECONDARY TO DECUBITUS ULCERS

In bedridden patients, prolonged soft-tissue ischemia from immobilization can lead to the formation of decubitus ulcers and subsequent osteomyelitis at pressure points. The ischium and calcaneus are common sites.

As with diabetic patients, cellulitis and reactive bone changes can mimic osteomyelitis on radiographs and radionuclide bone scans. Sugarman[53] studied twenty-eight patients with decubitus ulcers and found histologic evidence of osteomyelitis in only six out of fourteen patients where pressure sores exposed underlying bone. The clinical diagnosis of osteomyelitis was correct 60% of the time. Radiographs had a sensitivity of 50% and a specificity of 82%, and ^{99m}Tc-MDP bone scans had a sensitivity of 100% and a specificity of 50%. ^{67}Ga scans had a sensitivity of 83% and a specificity of 59%. Using histologic diagnosis as a gold standard, bone culture had a sensitivity of 100% but a specificity of only 33%. The low specificity resulted from contamination of cultures by organisms from the ulcers overlying the bone.

The use of MRI to diagnose osteomyelitis associated with decubitus ulcers has not been addressed in the literature. Given the difficulty of radiologic diagnosis in this setting, some advocate the use of bone biopsy for diagnosis.[53]

VI. BRODIE'S ABSCESS

Brodie's abscess is a subacute contained focus of infection within bone. It is most common in children but can also occur in adults. The abscess is usually metaphyseal in location and may cross the growth plate into the epiphysis.[54] While Brodie's abscess is usually caused by pyogenic bacteria (especially *Staphylococcus*), fungal infection may appear similar.

The patient may present with chronic pain, a limp, and local tenderness. Erythrocyte sedimentation rate and white blood cell count may be either normal or elevated. Brodie's abscess can often be treated with antibiotics, but surgical drainage may be required.

Plain radiographs are usually diagnostic for Brodie's abscess. Radiographs may be supplemented by CT scanning if the diagnosis is in question. The abscess appears as a well-defined lytic lesion surrounded by a thick rind of sclerotic reactive bone (Figures 10 and 11). The inner margin of this rind is sharply defined, while the outer margin fades gradually into normal bone. In contrast to the Brodie's abscess, other benign lytic lesions of bone such as fibrous dysplasia, enchondroma, chondroblastoma, and nonossifying fibroma

generally have a thin margin of sclerosis that is well defined on both the inner and outer aspects. Osteoid osteoma has a thick rind of reactive sclerotic bone, but the lucent portion of the lesion is usually limited to cortical bone and is much smaller than the Brodie's abscess.

VII. CHRONIC OSTEOMYELITIS

An untreated or inadequately treated episode of acute osteomyelitis can progress to chronic osteomyelitis. This scenario is rare today and most commonly, a chronic, indolent infection develops in an area of ischemic bone following fracture. The vascular supply is poor in the distal tibia, and chronic osteomyelitis is not uncommon following open tibial fracture. In the past *Staphylococcus aureus* was the most common inoculating organism, but there has been increasing incidence of Gram-negative anaerobic and mixed infections.[55,56]

Patients present with chronic pain and usually have an elevated erythrocyte sedimentation rate. The white blood cell count may be normal. Chronic osteomyelitis is generally treated with surgical debridement, and soft-tissue flaps may be needed to cover the wound. Some cases require amputation.[55,56]

Detection of active osteomyelitis may be difficult when bony abnormalities from fracture or a prior episode of osteomyelitis are present (Figure 12). Tumeh and colleagues[57] found that only one radiographic sign, the presence of a sequestrum, was specific for active infection. A sequestrum was, however, visible in only 9% of cases on plain radiographs. Bone erosion, periosteal reaction, and soft-tissue swelling are not accurate indicators of active disease. Progressive changes on serial radiographs have a sensitivity of 14% for active disease and a specificity of 70%.[57]

Used in isolation from other imaging studies, ^{99m}Tc-MDP bone scans are not useful for detecting chronic osteomyelitis associated with underlying bone abnormalities.[16,58] ^{67}Ga scanning has been used, but its accuracy is low.[16,58] Although ^{67}Ga scans may be normal in patients with active osteomyelitis,[59] ^{67}Ga uptake more intense than that of ^{99m}Tc-MDP is an accurate sign of osteomyelitis superimposed on other bone pathology.[59]

Indium scanning can be useful in diagnosing chronic osteomyelitis. A sensitivity of 94% and a specificity of 80% have been reported in the peripheral skeleton, but the accuracy is lower in the central skeleton.[20] One study of eight patients with chronic infection found indium to be less sensitive than ^{67}Ga;[60] however, a large study found a sensitivity of 86% for indium scans.[61]

If surgical treatment of chronic osteomyelitis is to be successful, sequestra must be resected. CT is more sensitive to identification of sequestra than plain radiography,[31] and therefore is quite useful in planning treatment. Conventional tomography (Figure 12) or MRI can also be used to detect sequestra.[35,62] An uncontrolled study found that MRI accurately depicted sequestra and sinus tracts in eight patients with chronic osteomyelitis and identified the extent of infection.[62]

Further work is needed in this area to define the sensitivity and specificity of MRI when compared with CT for detection of sequestration.

Sclerosing osteomyelitis of Garre is a chronic infection characterized by bony sclerosis (Figure 13). This diagnosis is extremely rare today, and osteosarcoma or sclerosing Ewing's sarcoma should be considered in the differential diagnosis.

VIII. CHRONIC MULTIFOCAL OSTEOMYELITIS

Chronic multifocal osteomyelitis (CMFO) is a rare condition that is seen in children and adolescents. It is also known as plasma cell osteomyelitis, chronic recurrent multifocal osteomyelitis, chronic symmetric plasma cell osteomyelitis, and primary chronic osteomyelitis. The etiology of CMFO is unclear, and organisms are usually not recovered from the lesions. Histology demonstrate fibrosis and plasma cells.[63,64]

CMFO primarily affects the medical end of the clavicle and the metaphyses of long bones around the knee. Patients present with pain, and the erythrocyte sedimentation rate is mildly to moderately elevated.[65] A skin rash, palmoplantar pustulosis, may be present.[66] Although only a single area may be affected initially, other lesions may develop at a later time. The lesions respond to treatment with nonsteroidal antiinflammatory drugs. Plain radiographs typically reveal a lytic lesion that is often small and lacks significant surrounding sclerosis[65] (Figure 14).

IX. OSTEOMYELITIS IN CHILDREN

The most common presentation of osteomyelitis in childhood is fever with limb pain and tenderness over the metaphysis of the bone. Neonates present with fever and will not move the affected limb. Infection in children is usually limited to the metaphysis of the bone, but infection in the neonate often spreads to the epiphysis and joint. This distinction can be ascribed to the differences in bone vascularity discussed previously. Epiphyseal infection can, however, be seen in older children.[67] In young children, osteomyelitis can occasionally result in growth disturbance.[68]

Staphylococcus aureus remains the most common causative organism in childhood osteomyelitis. In children under the age of 2 years, hemophilus influenzae causes approximately 20% of cases of osteomyelitis.[69,70]

The diagnosis of osteomyelitis in children can be difficult. Plain radiographic changes develop slowly, and intense ^{99m}Tc-MDP uptake at normal growth plates can result in false-negative bone scans.[13,71–73] ^{67}Ga scans can be used to increase sensitivity but at the cost of decreased specificity.[74] MRI will reveal marrow changes, but sedation is needed for imaging the young patient. Clinical diagnosis early in the course of the infection is probably more reliable than plain radiographic

diagnosis.[69] Biopsy may be needed to isolate the pathogen and/or confirm the diagnosis.

X. SPINAL OSTEOMYELITIS

Predisposing factors for the development of spinal osteomyelitis include immune suppression, diabetes mellitus, chronic obstructive pulmonary disease, infection elsewhere (genitourinary infection, bacterial endocarditis), and recent surgery.[75,76] Spinal osteomyelitis has been reported as both a complication and a cause of mycotic aneurysms of the aorta.[77] This rare association is important to recognize because of the risk of rupture of the mycotic aneurysm.

A review of 43 patients with spinal osteomyelitis[75] found that 77% of the patients were older than 50 years. Ninety-eight percent presented with local spine pain that had been present for a mean duration of 6 weeks. Only 50% had fever, but all had an elevated erythrocyte sedimentation rate. *Staphylococcus aureus* is the most common infectious agent. Spinal tuberculosis (Pott's disease) remains a diagnostic consideration, especially in the immigrant or immunocompromised population.[76]

Vertebral osteomyelitis usually occurs by hematogenous seeding, which may be either arterial or less commonly venous via Batson's plexus. The lumbar spine is the most common site, followed by the thoracic spine. Infection is uncommon in the cervical spine. The infection initially develops in the anterior portion of a vertebral body, beneath the anterior longitudinal ligament where blood flow is slow. It may spread across the disk to an adjacent vertebral body. Spread into adjacent soft tissues may lead to abscess formation in the epidural space or psoas muscle. Epidural abscess from hematogenous seeding need not be associated with osteomyelitis.

Although the intervertebral disk is avascular in older adults, it can have a functional vascular supply through the third decade.[76] Primary infectious diskitis can thus occur in the younger population via the hematogenous route. Primary diskitis can also occur following diskectomy or other instrumentation, including diskography or chymopapain injection.[76]

Plain radiographs of vertebral osteomyelitis demonstrate osteoporosis and endplate erosion. Disk space narrowing is usually also present (Figure 15). A pronounced kyphosis (gibbus deformity) can develop in Pott's disease.

Nonenhanced CT can confirm bony destruction, and enhanced CT accurately defines soft-tissue abscess formation. MRI is also highly accurate for the diagnosis of spinal osteomyelitis[32,78] (Figure 15). Gadolinium administration may be useful to define the extent of bone and soft-tissue involvement and may assist in the diagnosis of epidural abscess when osteomyelitis is absent.[79]

Although combined ^{67}Ga and ^{99m}Tc-MDP bone scans have been reported to be accurate in the diagnosis of spinal osteomyelitis,[32] false-negative bone scans have

been reported in vertebral osteomyelitis in elderly adults.[80] These false-negative scans may be due to regional ischemia causing poor delivery of radionuclide to the affected region.

XI. INFECTIOUS ARTHRITIS

Infectious (septic) arthritis can occur as a result of a puncture wound, hematogenous seeding, or spread from adjacent cellulitis. Most cases of diabetic osteomyelitis have a component of septic arthritis.

The patient with infectious arthritis due to pyogenic bacteria presents with fever, arthralgia, and signs of local inflammation. Radiographs show a rapidly progressive arthritis with joint effusion, joint space narrowing, and bony erosions (Figures 16 and 17). Fungal or mycobacterial organisms have a more indolent course. When the diagnosis is suspected clinically and radiographs are normal, early joint aspiration is essential for gram stain and culture in order to allow initiation of appropriate treatment.

XII. SOFT-TISSUE INFECTION

Soft-tissue infections may consist of diffuse cellulitis that can be treated medically, or focal abscess that generally requires drainage in addition to antibiotics. Soft-tissue infections present with the classic signs of inflammation: redness, heat, pain, and swelling. An abscess in a deep, muscular compartment may be clinically occult.

On plain radiographs, soft-tissue swelling and obscuration of soft-tissue planes are often evident. The three-phase bone scan usually demonstrates increased flow and blood pool activity in the affected area, but decreasing activity is evident on delayed images.[7,8] Both MRI and CT are useful for diagnosing soft-tissue abscesses. The abscess cavity will be low attenuation on CT. With MRI, the abscess will show low signal intensity on T1-weighted images, and high signal intensity on T2-weighted images. The abscess wall will enhance with contrast on both CT and MRI (Figure 18). Whereas this pattern is highly suggestive of abscess, other soft-tissue masses, including seroma or necrotic sarcoma, can show identical findings.[81]

SUMMARY

Establishing the diagnosis of osteomyelitis may not present a clinical challenge in cases where classic plain radiographic changes are found in the appropriate clinical setting. Often, however, additional imaging with radionuclide scans, MRI or CT is necessary. The choice of imaging modality will reflect the age of the

patient, the location of suspected infection, and the presence of underlying bony abnormalities. Correlation of different imaging studies may be necessary to improve specificity. Biopsy may be required in challenging cases or for isolation of the offending organism.

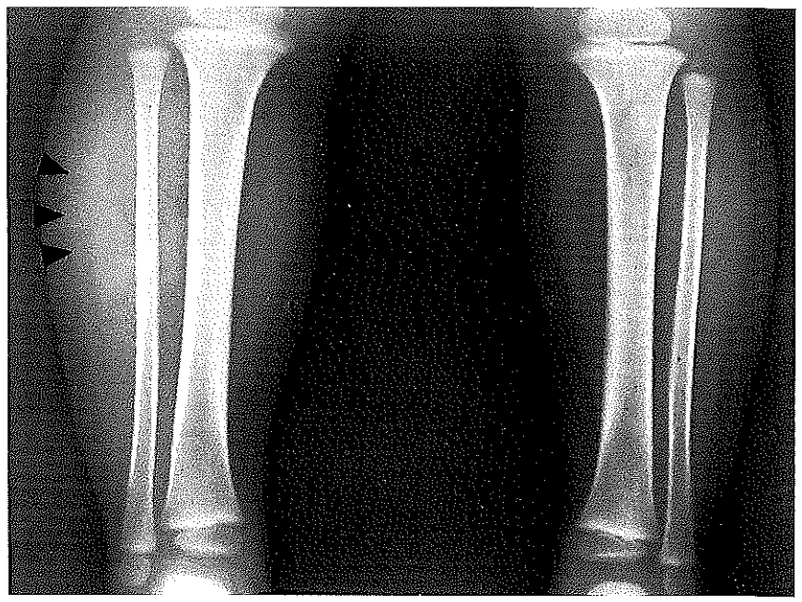

A

FIGURE 1. Osteomyelitis of the fibula in a young child. (A) Initial AP radiograph demonstrates soft-tissue edema and blurring of soft-tissue planes (arrowheads). (B) Follow-up AP radiograph demonstrates sequestrum formation (open arrow), surrounded by an involucrum of periosteal new bone (solid arrow).

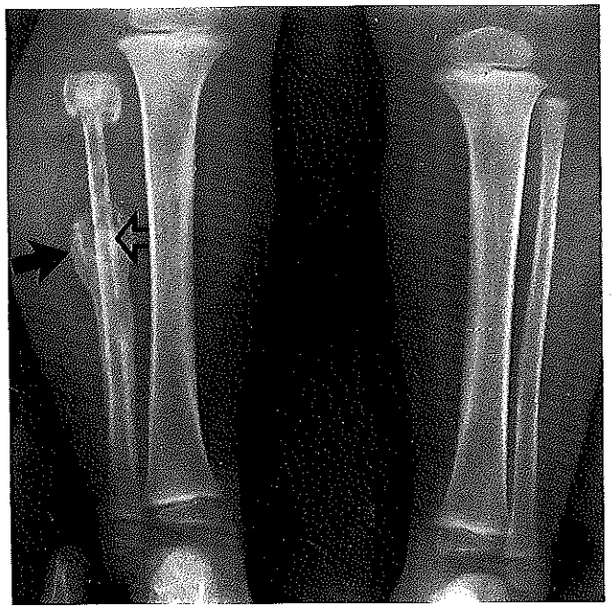

FIGURE 1B

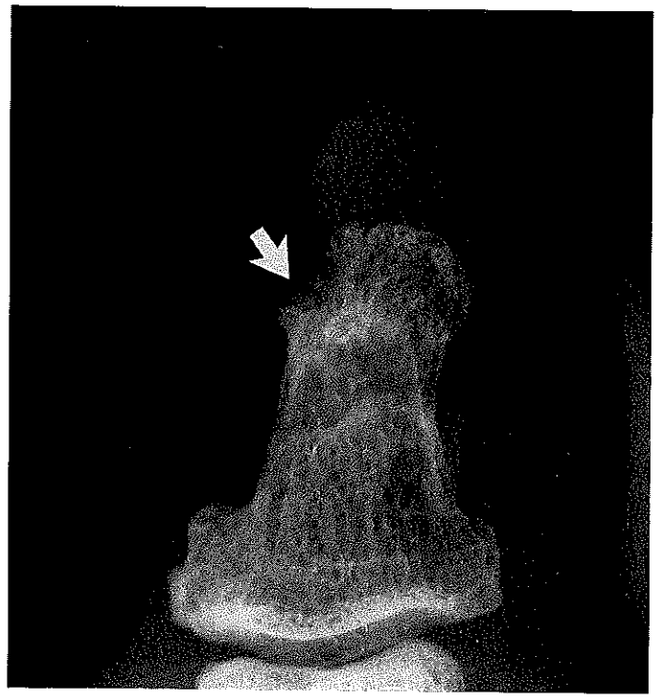

A

FIGURE 2. Osteomyelitis of the first distal phalanx. (A) Initial radiograph demonstrates subtle cortical erosion of the ungual tuft (arrow). The patient was not treated. (B) Ten days later, progressive destruction is seen.

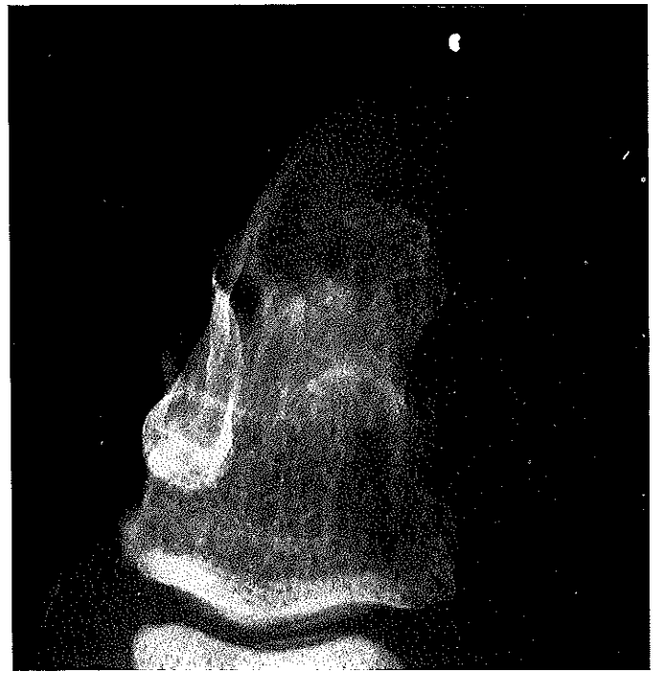

FIGURE 2B

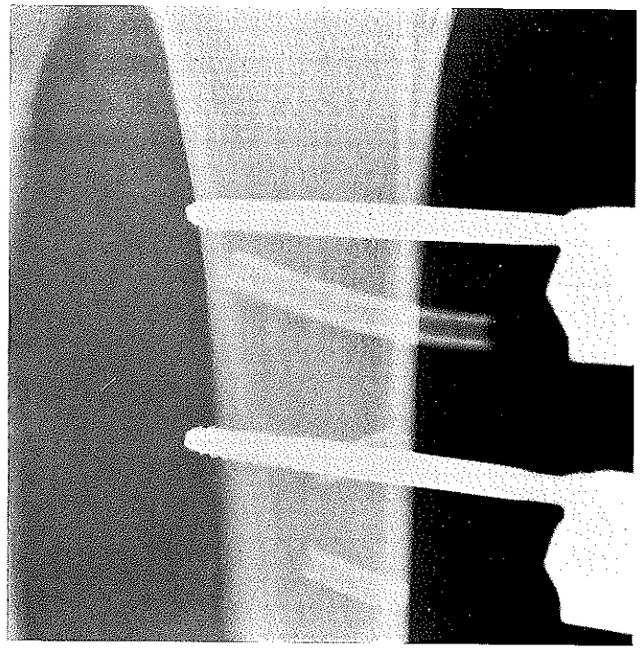

A

FIGURE 3. Tibial osteomyelitis occurring at site of external fixator pins. (A) Baseline AP radiograph shows normal bone density surrounding pins. (B) Follow-up radiograph shows poorly marginated lucencies at pin sites. (C) Lateral radiograph shows that the lucencies are round in shape and located primarily anteriorly.

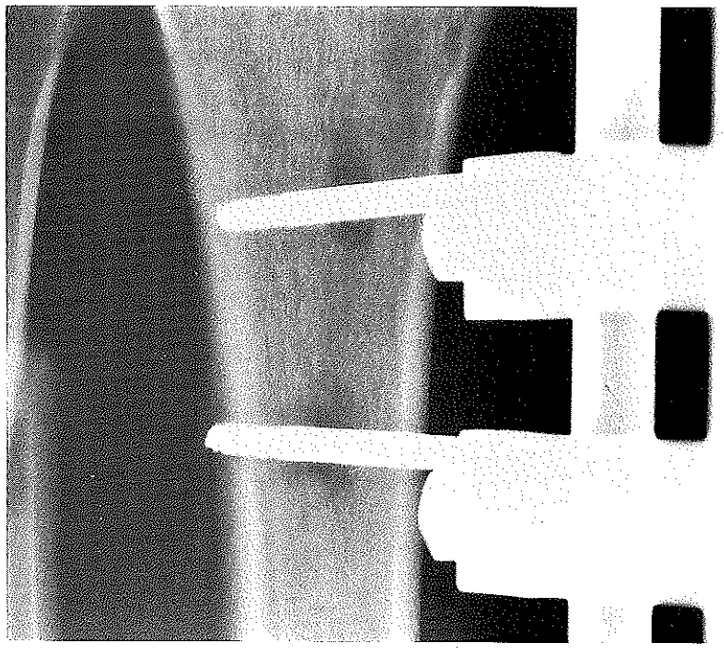

FIGURE 3B

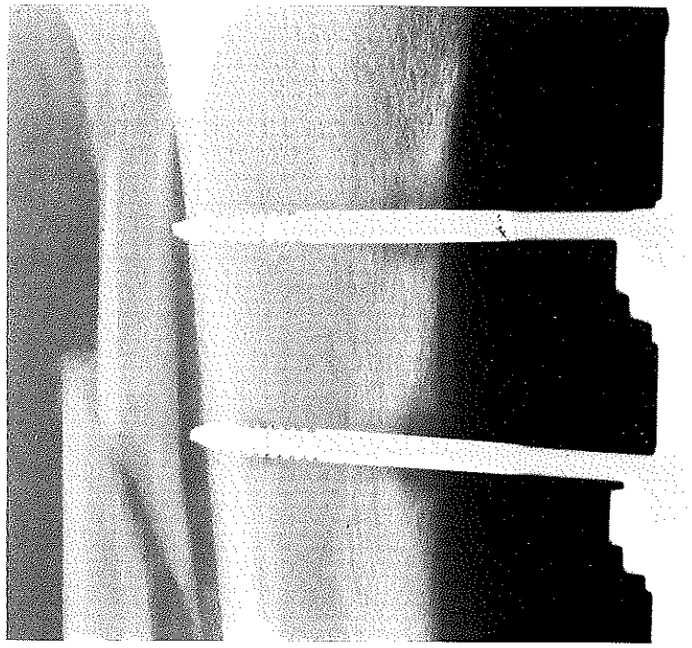

FIGURE 3C

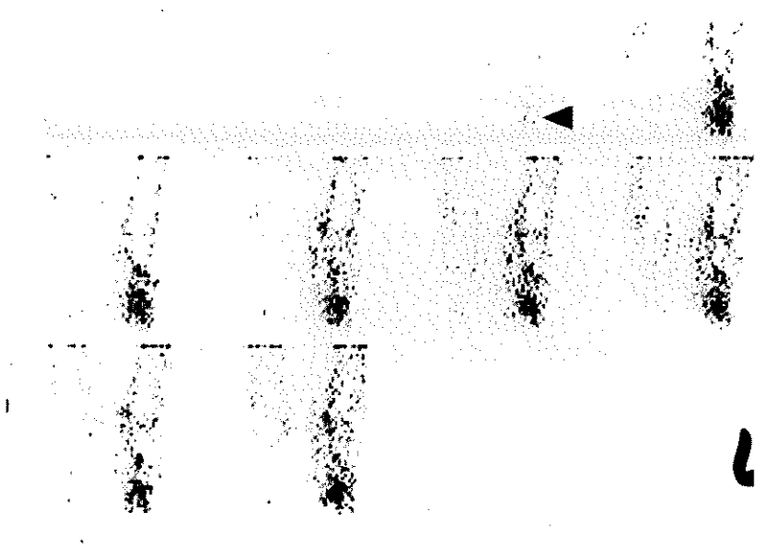

A

FIGURE 4. Osteomyelitis diagnosed by three-phase technetium bone scan (A–C) and indium scan (D). Plain radiographs were normal. (A) Images obtained every four seconds following injection of ^{99m}Tc-MDP demonstrate increased arterial flow to the second or third metatarsal of the left foot, evident on the first image (arrow) and becoming more prominent over time. (B) Blood pool image shows diffusely increased activity in this region (arrow). (C) Delayed image shows increasing localization of activity in the second metatarsal head (arrow). Note that there is prominent activity in several other areas, on the delayed image. Because these areas show normal blood flow, infection there is excluded. Plain radiographs showed degenerative changes in these areas. (D) ^{111}In WBC scan in the same patient shows a focus of intense activity (arrow) at the second metatarsal head. Note that spatial resolution is poor when compared with the ^{99m}Tc-MDP scan.

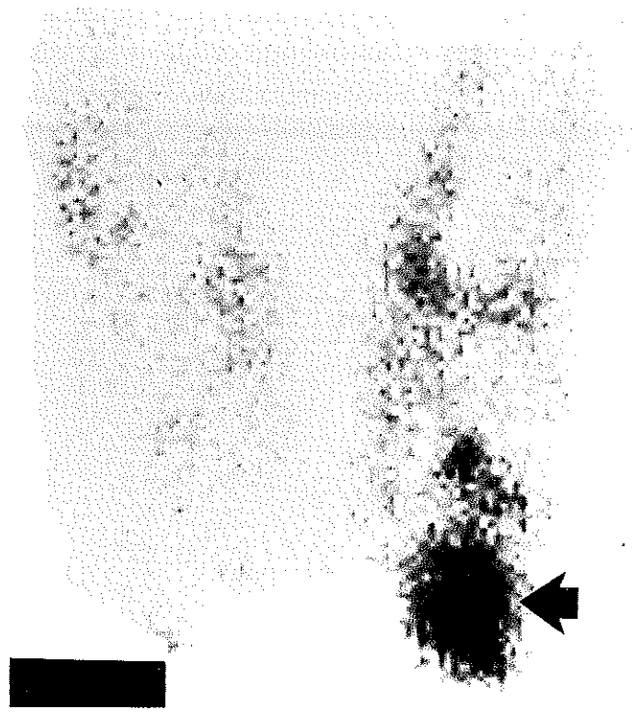

FIGURE 4B

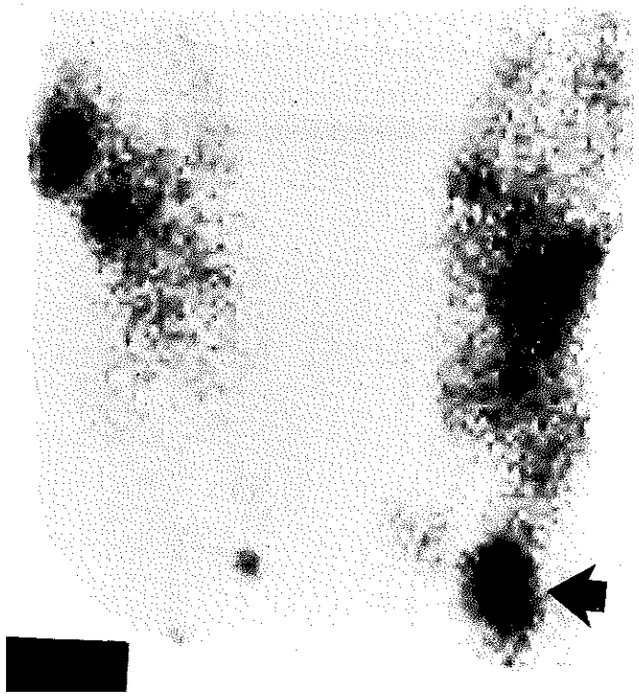

FIGURE 4C

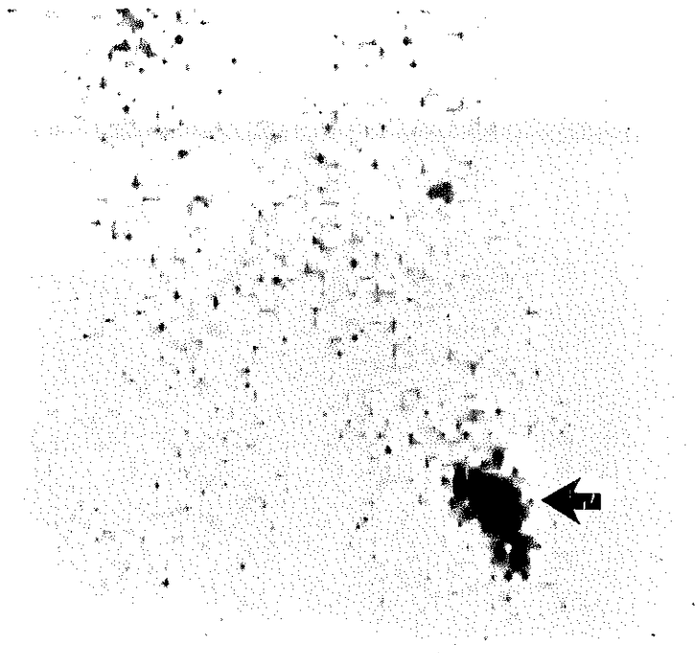

FIGURE 4D

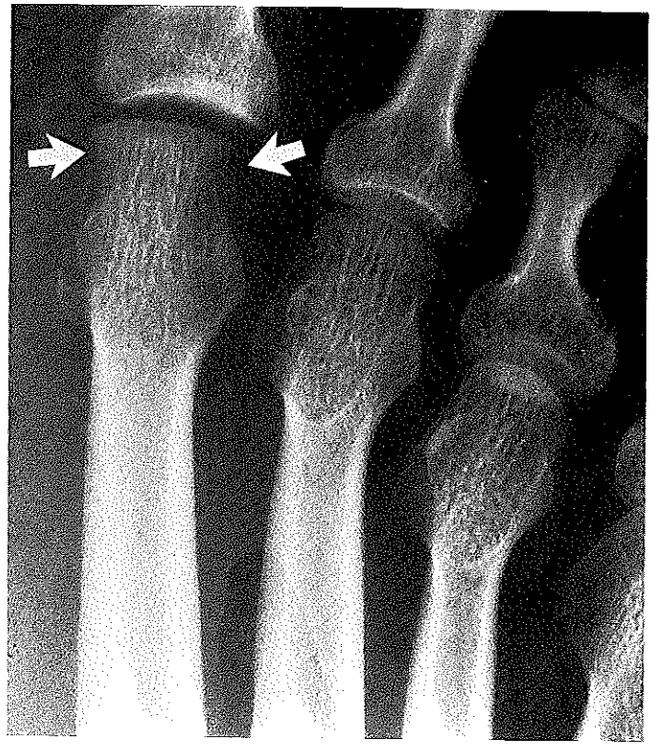

A

FIGURE 5. Osteomyelitis of the second metatarsal head. (A) Plain radiograph shows very subtle loss of cortical bone (arrows) compared with third and fourth metatarsal heads. (B) Coronal SE T1-weighted MRI (SE 600/18). The normal high signal intensity fatty bone marrow has been replaced with low signal intensity pus in the second metatarsal head, and cortical erosion is evident (arrow). Cellulitis surrounding the metatarsal head is also low signal intensity. (C) Coronal FSE T2-weighted (SE 4000/104). Normal fatty marrow has decreased in signal intensity, while the purulent marrow in the second metatarsal and surrounding cellulitis have very high signal intensity. (D) Sagittal STIR image (SE 2367/40/155). The difference between low signal intensity normal marrow (white arrow) and high signal intensity abnormal marrow (black arrow) is exaggerated. Joint distension from septic arthritis (open arrow) can be appreciated.

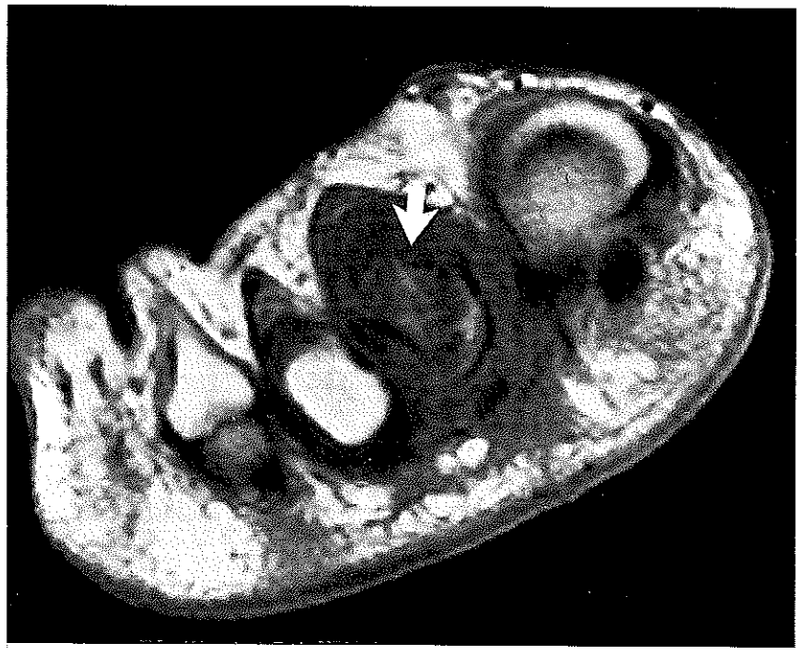

FIGURE 5B

FIGURE 5C

FIGURE 5D

A

FIGURE 6. Multiple infarctions in patient on chronic steroid medication. (A) Coronal proton density image (SE 2000/20) shows well-defined foci of abnormal signal intensity involving the distal femur and proximal tibia bilaterally, left greater than right. Areas of involvement are sharply demarcated and have a serpentine border. (B) Coronal T2-weighted image (SE 2000/80). The infarctions are heterogeneous, with areas of both high- and low signal intensity.

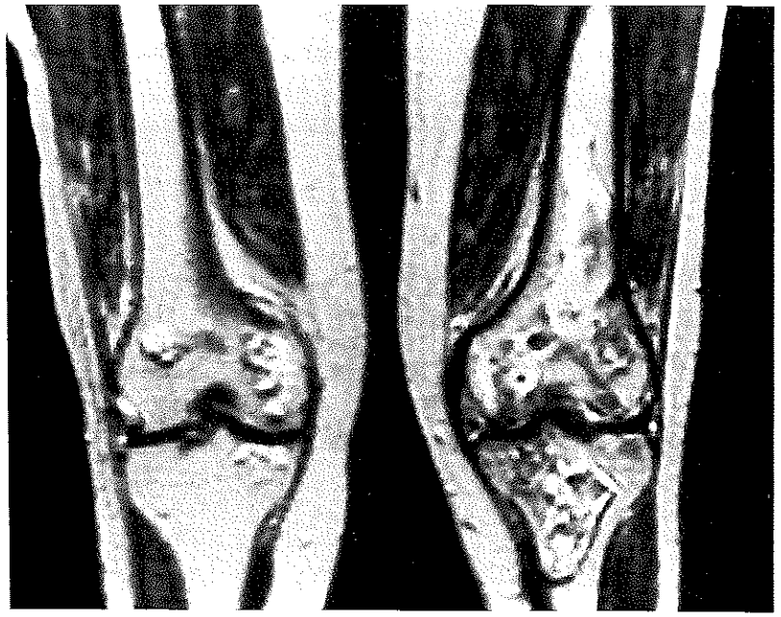

FIGURE 6B

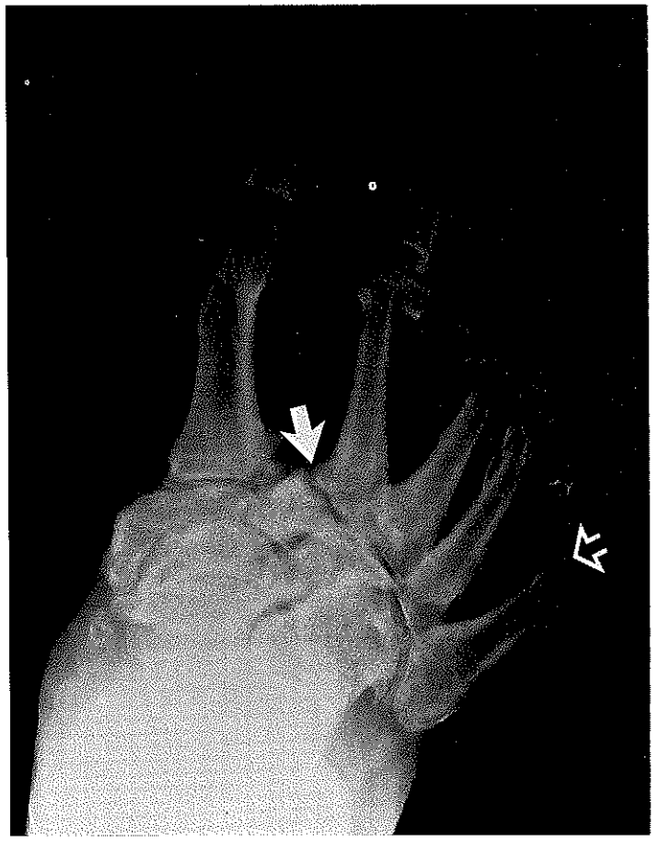

FIGURE 7. Neuroarthropathy involving the naviculocuneiform, Lisfranc and metatarsophalangeal joints. There is bone proliferation and debris in the midfoot (arrow), but changes are primarily resorptive changes at the metatarsophalangeal joints (open arrow). Characteristic of neuropathic joints, bone density is preserved. Prominent periosteal new bone along the metatarsal shafts should not be mistaken for a sign of infection. Deformity of the first metatarsal head is from prior bunionectomy.

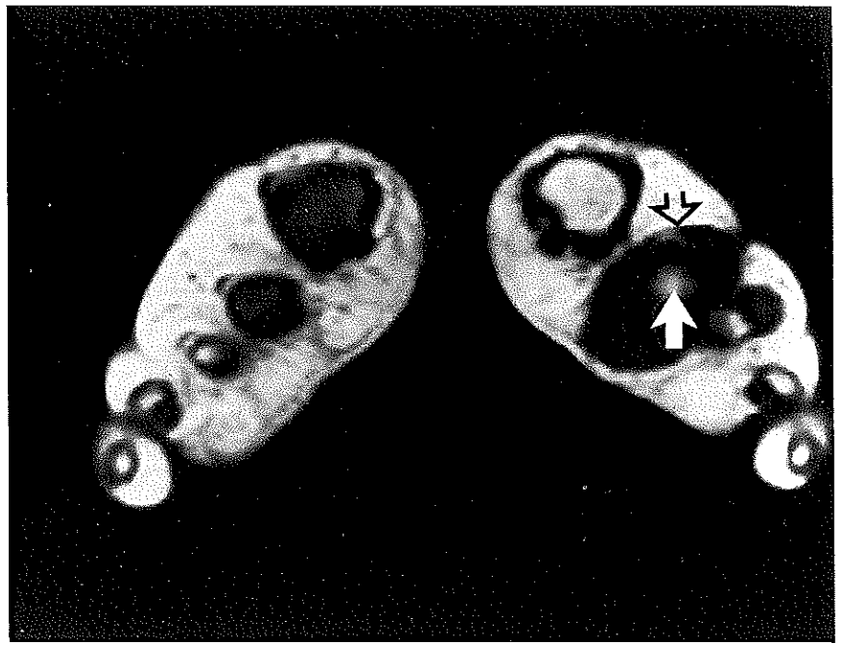

FIGURE 8. Cellulitis surrounding the second metatarsal shaft. Three-phase bone scan was false-positive for osteomyelitis. Coronal T1-weighted MRI (SE 560/20) reveals normal marrow signal intensity (arrow). Cellulitis (open arrow) surrounds the shaft. The low signal intensity on the right reflects partial volume averaging through the metatarsophalangeal joints.

Decision Tree for Diagnosis of Diabetic Osteomyelitis

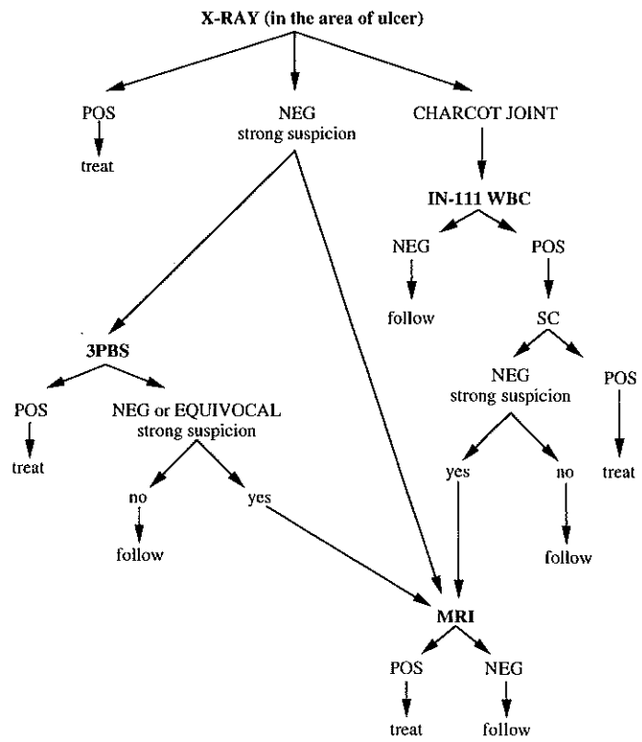

FIGURE 9. Decision tree for imaging diagnosis of osteomyelitis in the diabetic population. In WBC = indium-labeled white blood cell scan, 3PBS = three-phase bone scan, SC = technetium-sulfur colloid scan.

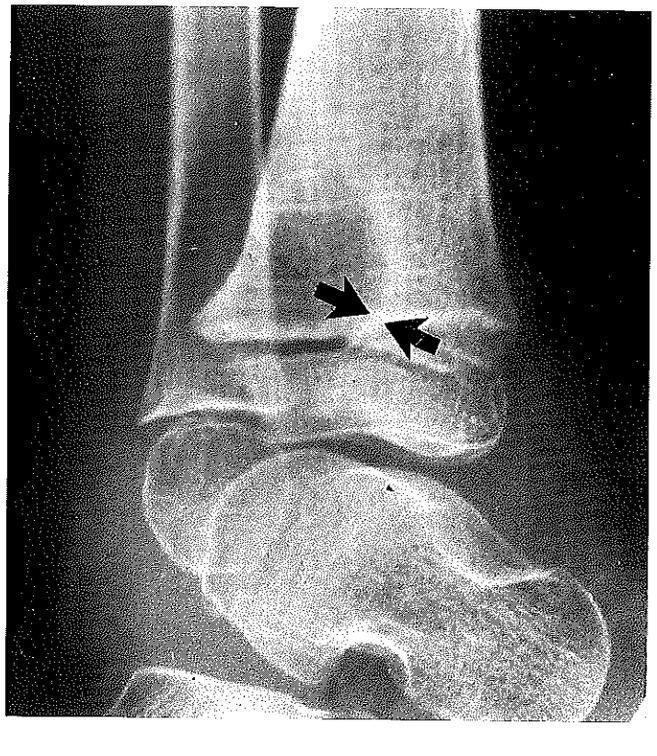

A

FIGURE 10. Five-year-old girl with Brodie's abscess. (A) Lateral plain radiograph shows a lytic metaphyseal lesion with a thick, sclerotic border (arrows). The outer margin of the border is ill defined, while the inner margin is sharp. (B) Axial CT better demonstrates the thick sclerotic rind (arrow) surrounding the lesion. Additional images showed that the abscess crossed the physeal plate into the epiphysis, a finding that was not appreciated on plain radiographs.

FIGURE 10B

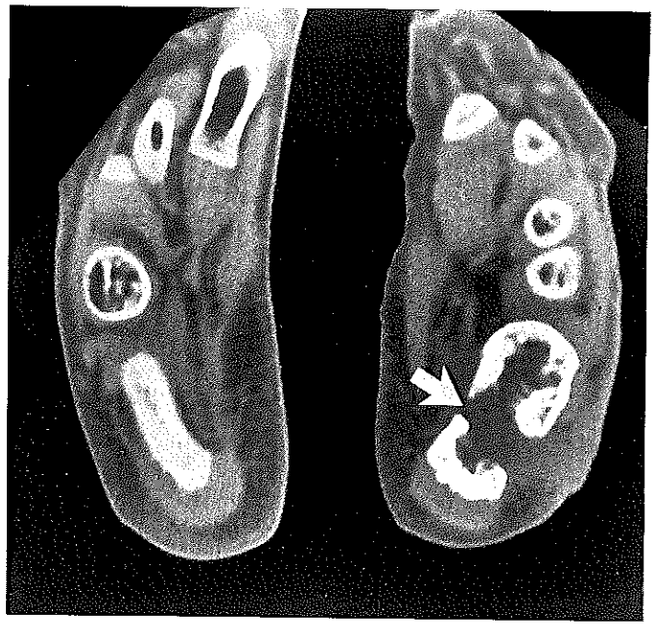

FIGURE 11. One-year-old child with coccidiomycosis infection of the calcaneus, hematogenous spread following pulmonary infection. Axial CT. The normal marrow has been replaced with soft-tissue density of purulent exudate. A sinus tract has developed medially (arrow). The lateral wall defect is postsurgical.

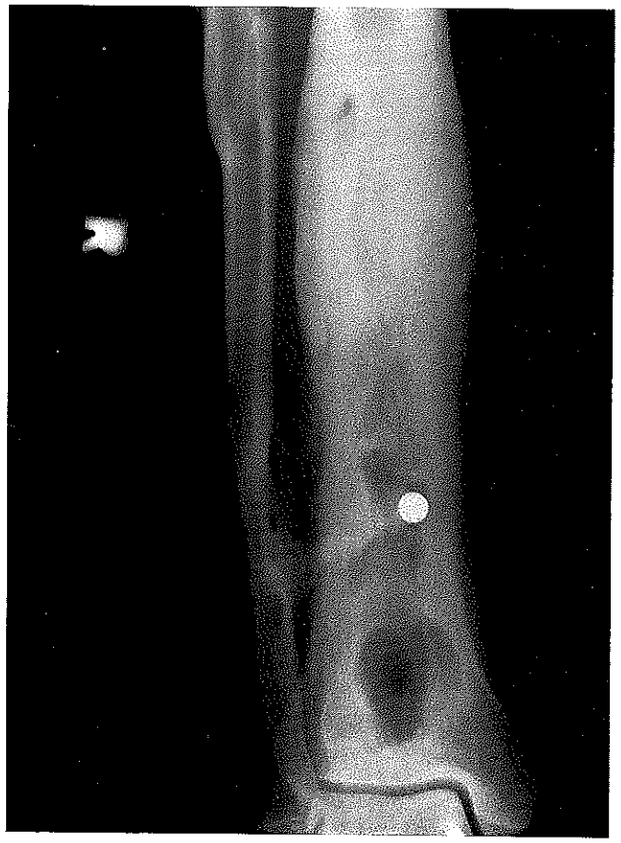

A

FIGURE 12. Chronic osteomyelitis following gunshot wound. (A) AP radiograph shows sclerosis proximally, a retained shot pellet, and a lucent cavity distally. (B) AP complex motion tomography shows bony sequestrum (arrow). The more inferior cavity was sterile.

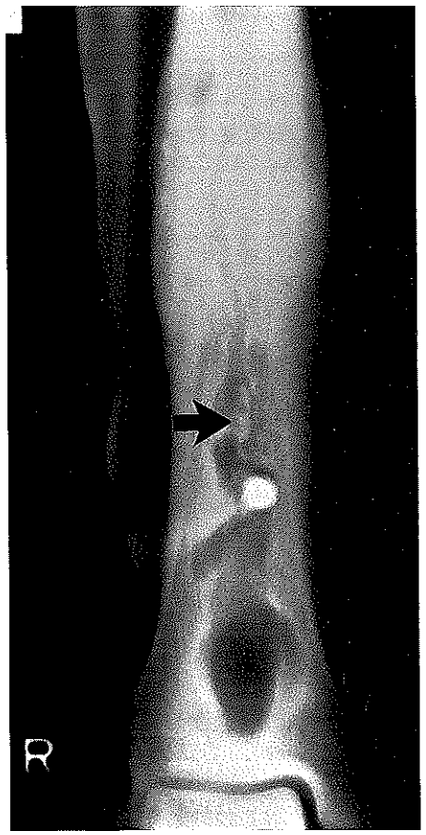

FIGURE 12B

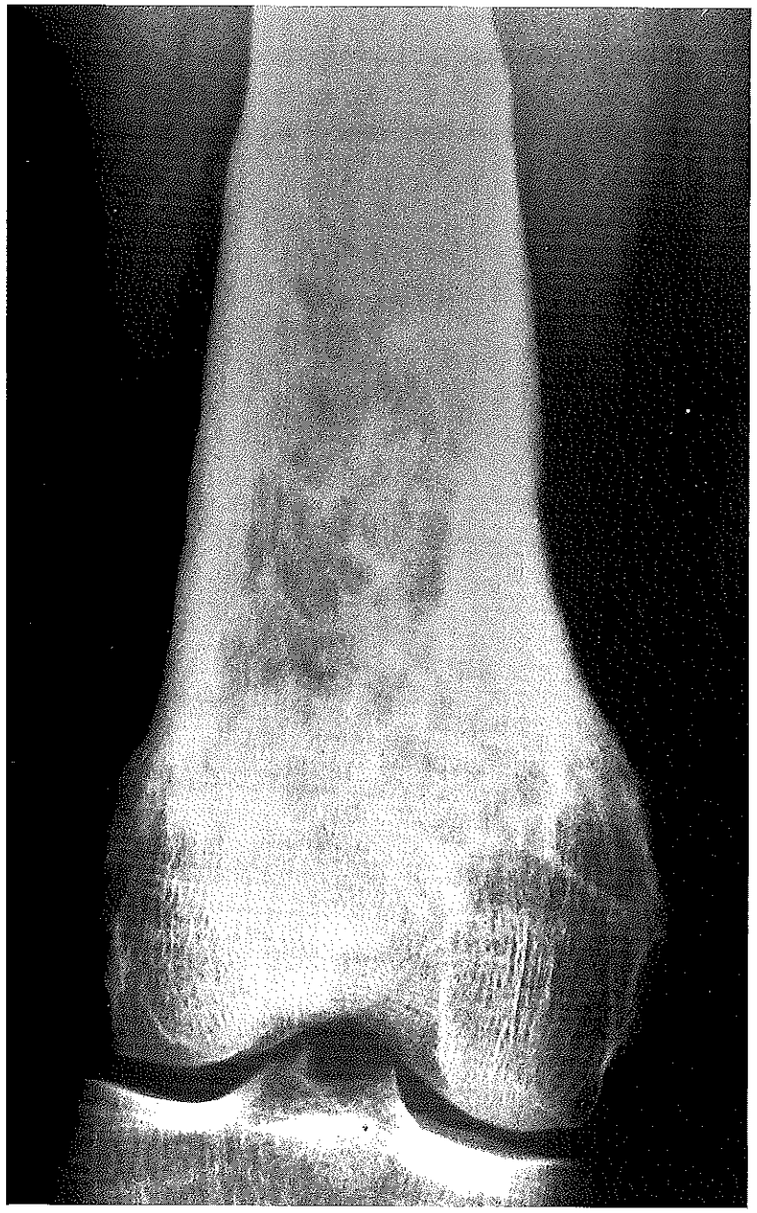

A

FIGURE 13. Sclerosing osteomyelitis of Garre. AP radiograph. The cortex is markedly thickened and irregular, and bone is expanded.

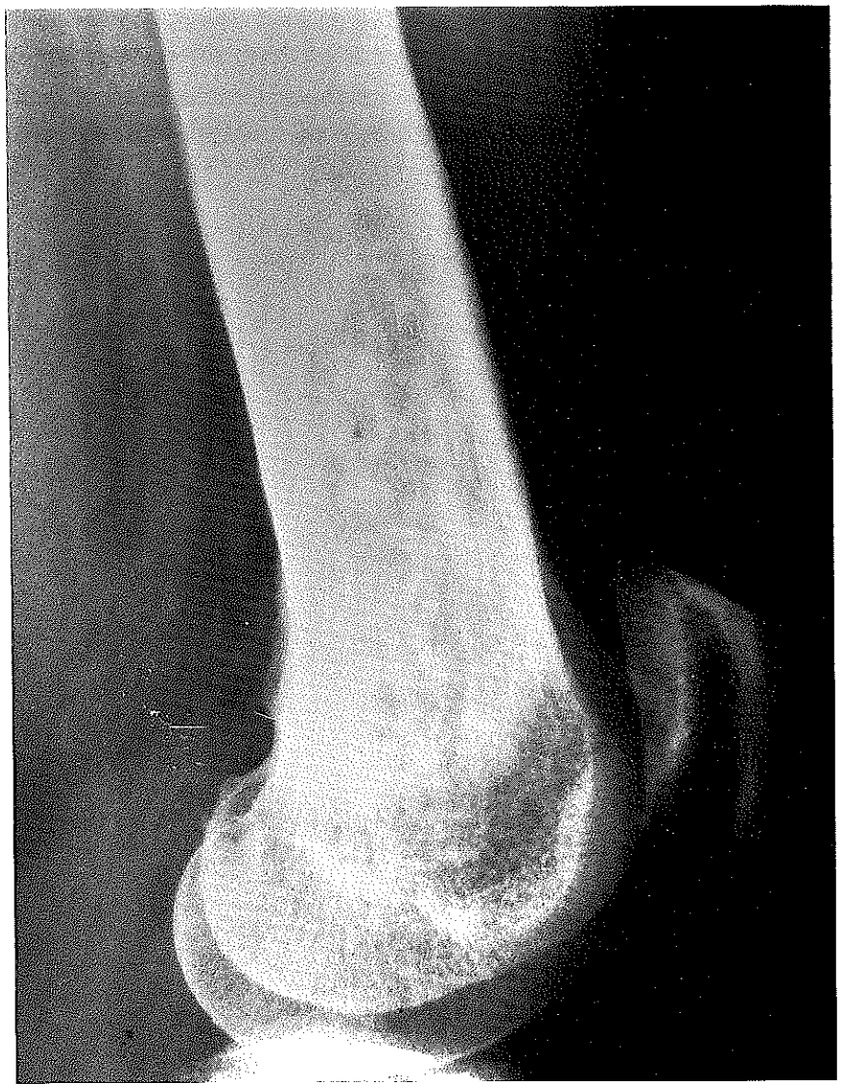

FIGURE 13B

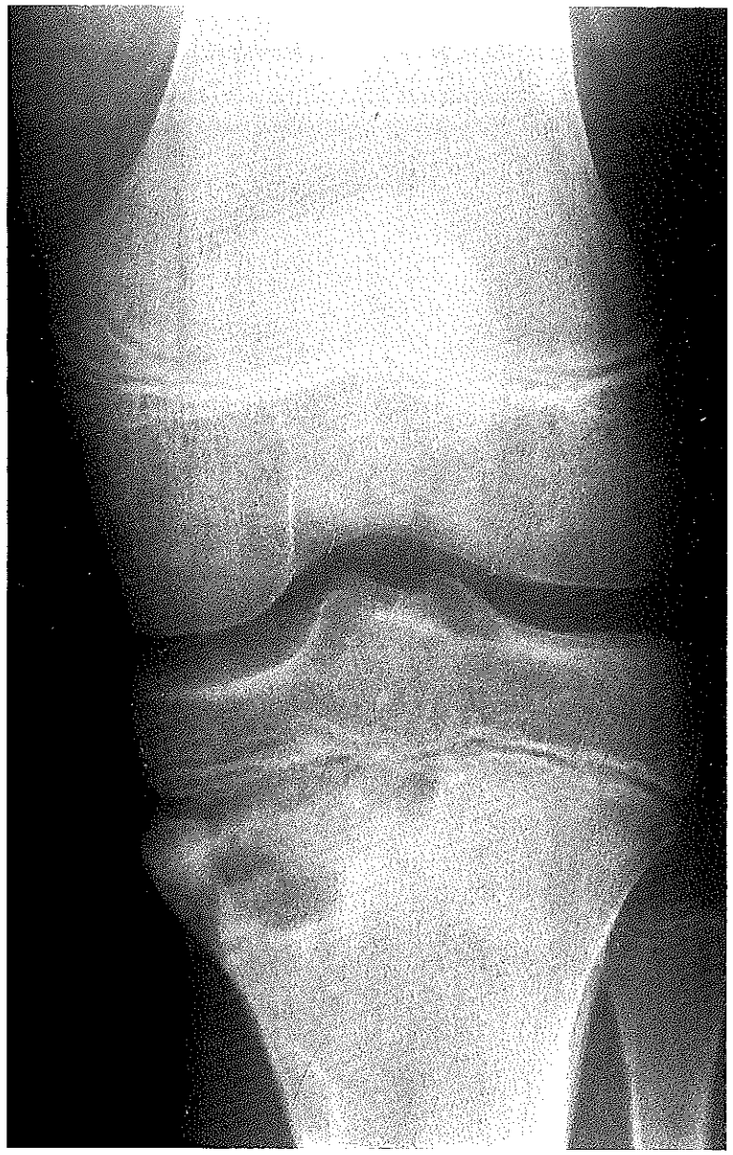

A

FIGURE 14. Chronic multifocal osteomyelitis. (A) AP radiograph of knee demonstrates an irregularly shaped lucency adjacent to the physis. Histology was determined to be "nonspecific". (B) CT of clavicle 4 years later shows a destructive process involving the cortex and subcortical bone of the right medial clavicle. Note that the sternal articular surface is normal. This finding excludes an infectious arthritis.

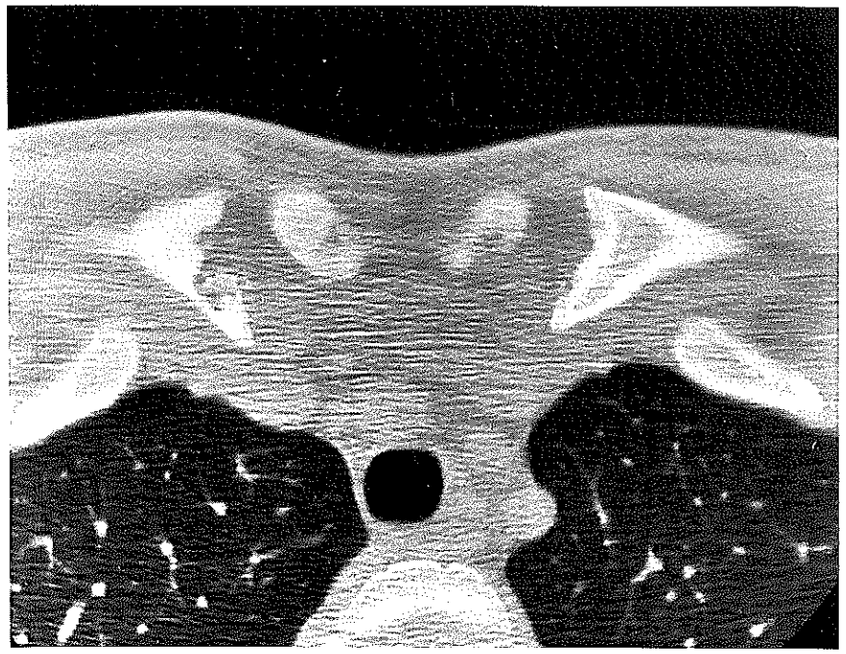

FIGURE 14B

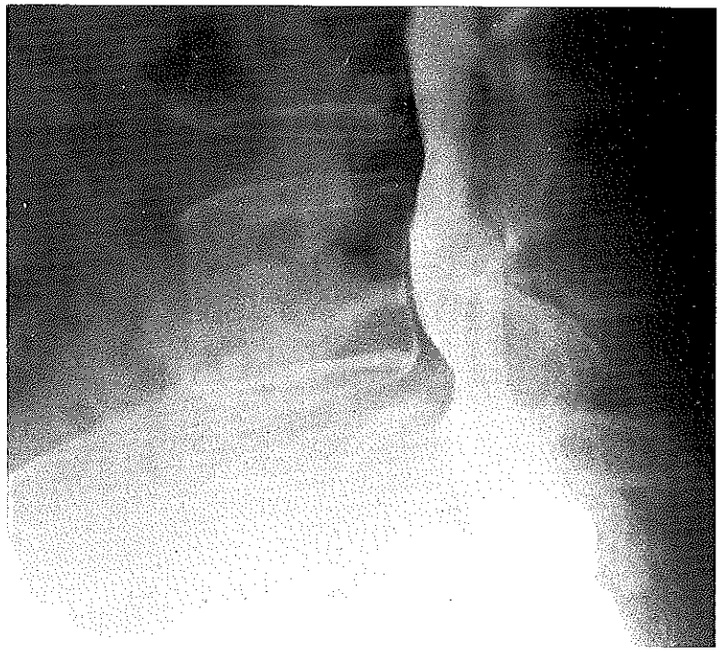

A

FIGURE 15. Post-diskectomy osteomyelitis of the spine. (A) Preoperative lateral radiograph obtained during myelography. There is an end-plate compression fracture of L5 that appears mature. (B) Radiograph 6 weeks following diskectomy. There is loss of the "white line" of the inferior and anterior cortex of L4 and superior cortex of L5 (arrows). (C) Nonenhanced axial SE T1-weighted MRI (SE 560/20) 3 weeks following surgery. Nonspecific intermediate signal intensity in spinal canal (arrows) could represent recurrent disk, postoperative edema, or infection. (D) Gadolinium-enhanced SE T1-weighted MRI (SE 560/20) obtained at the same time. There is enhancement of the majority of the tissue in the canal. This was felt to represent postoperative edema and early fibrous tissue. In actuality, it represented infection. Enhancement in the right psoas muscles (arrow) is a clue to the presence of infection. The left psoas is atrophic, a finding not related to the current infection. (E) Nonenhanced sagittal SE T1-weighted MRI (SE 580/20) 6 weeks following surgery shows diffuse loss of marrow signal throughout the L4 and L5 vertebral bodies. The epidural mass has increased in size from the previous MRI. (F) Gadolinium-enhanced sagittal SE T1-weighted MRI (SE 580/20). The epidural mass enhances diffusely. Biopsy at this time demonstrated staphylococcal infection.

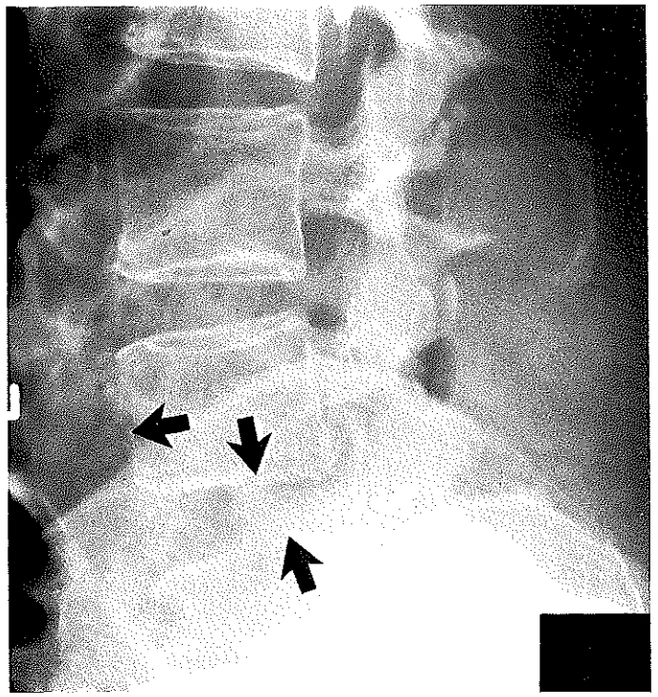

FIGURE 15B

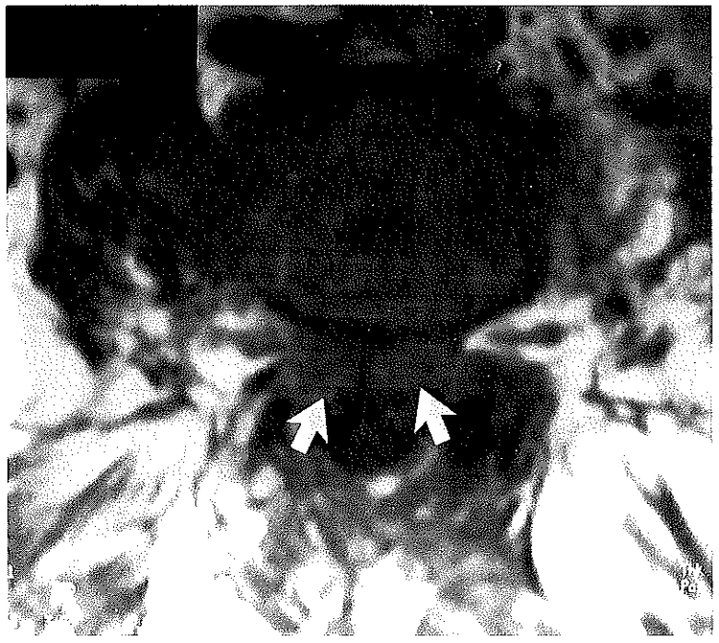

FIGURE 15C

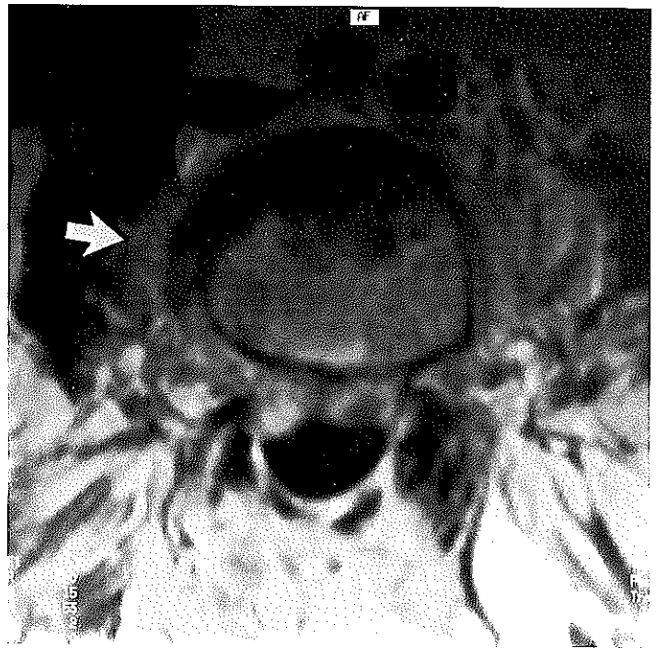

FIGURE 15D

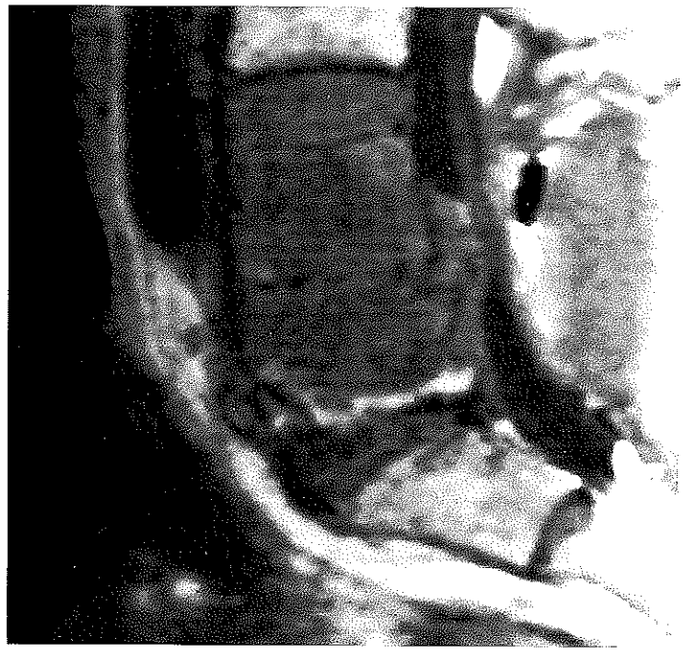

FIGURE 15E

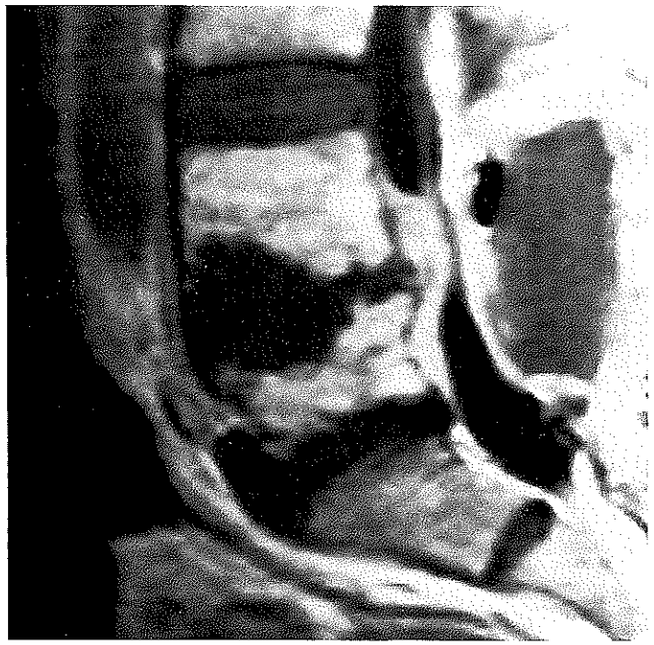

FIGURE 15F

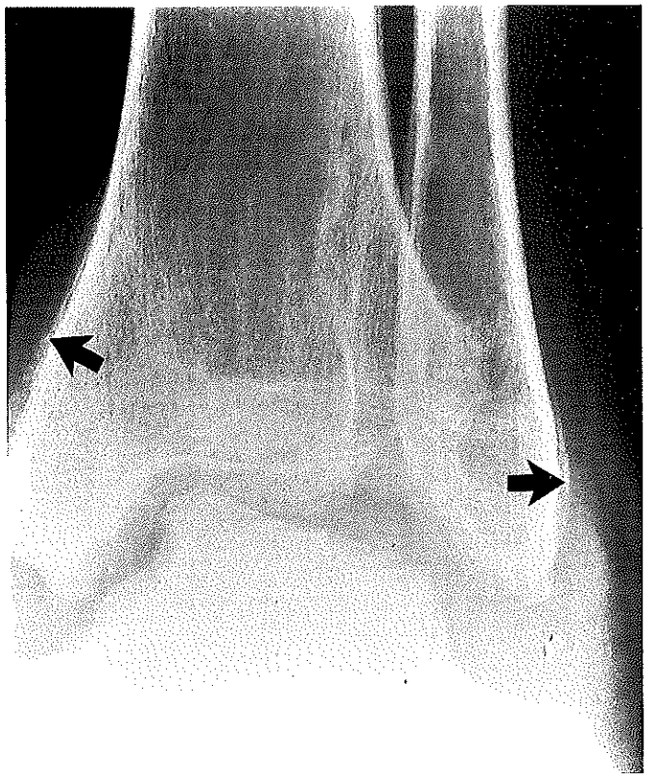

A

FIGURE 16. Septic arthritis of the ankle. (A) AP radiograph. The bones are osteoporotic, and erosions and joint distension are seen. Periosteal new bone is seen along the shafts of the tibia and fibula (arrows). (B) Lateral radiograph. Communication between the subtalar joint and the ankle joint resulted in marked narrowing of the subtalar joint (arrow) due to articular cartilage destruction.

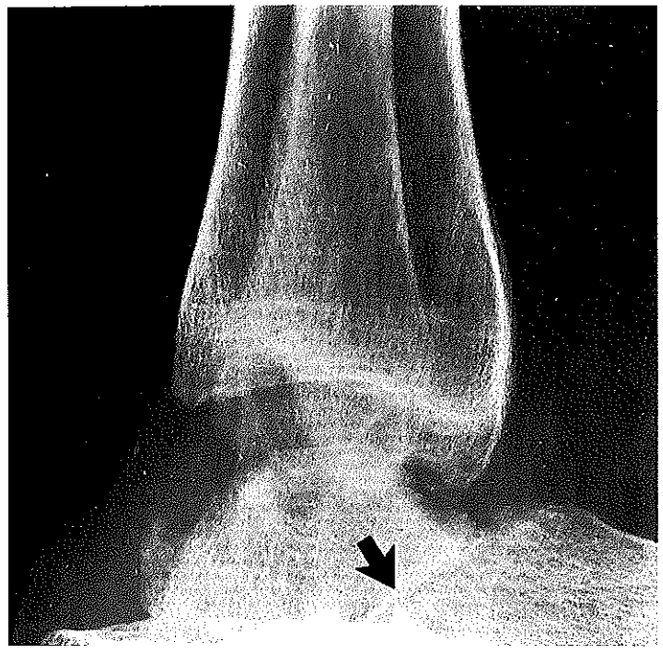

FIGURE 16B

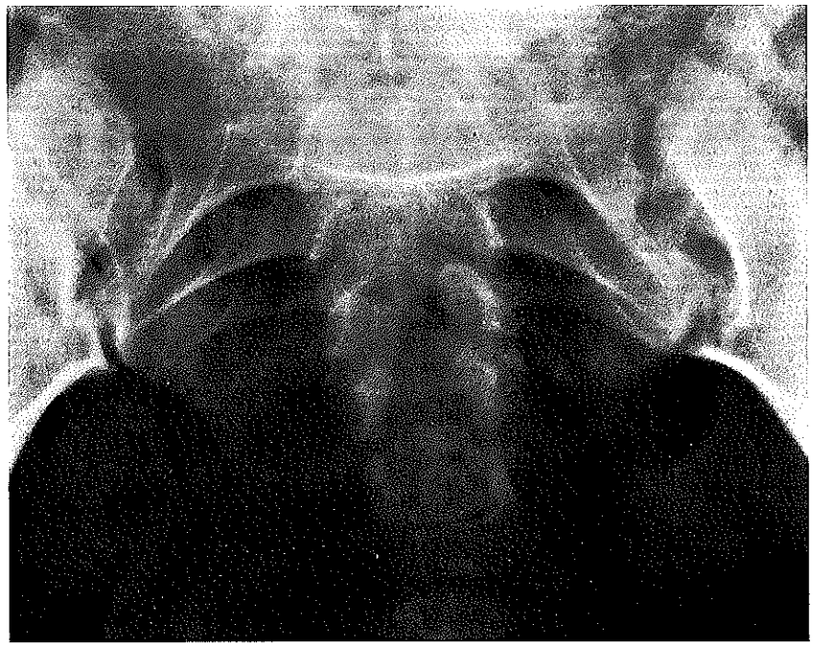

A

FIGURE 17. Septic arthritis of the left sacroiliac joint. (A) Plain radiograph shows widening and loss of cortical definition at the inferior aspect of the left sacroiliac joint (arrow). (B) These findings (arrows) are clearly seen on CT performed at time of biopsy.

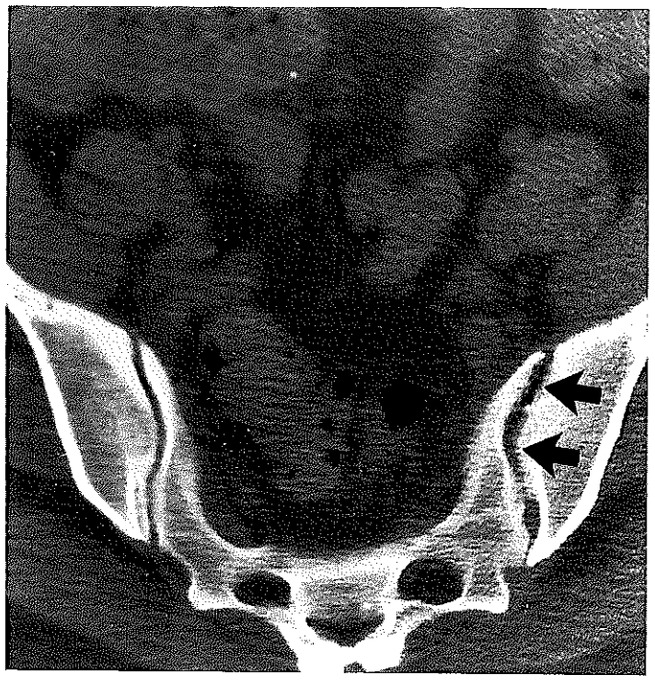

FIGURE 17B

A

FIGURE 18. Right thigh abscess. (A) Axial T1-weighted MRI (SE 500/20) shows a mass in the adductor magnus (arrow). The rim is of slightly higher signal intensity than the necrotic center. (B) Gadolinium-enhanced axial SE T1-weighted MRI (SE 500/20) with fat suppression. The rim of the abscess shows marked enhancement, while the necrotic center does not. (C) Coronal SE T2-weighted MRI (SE 2000/80). The entire mass, as well as surrounding edema are high signal intensity. Hematoma, seroma, or necrotic tumor may show the same MRI appearance.

FIGURE 18B

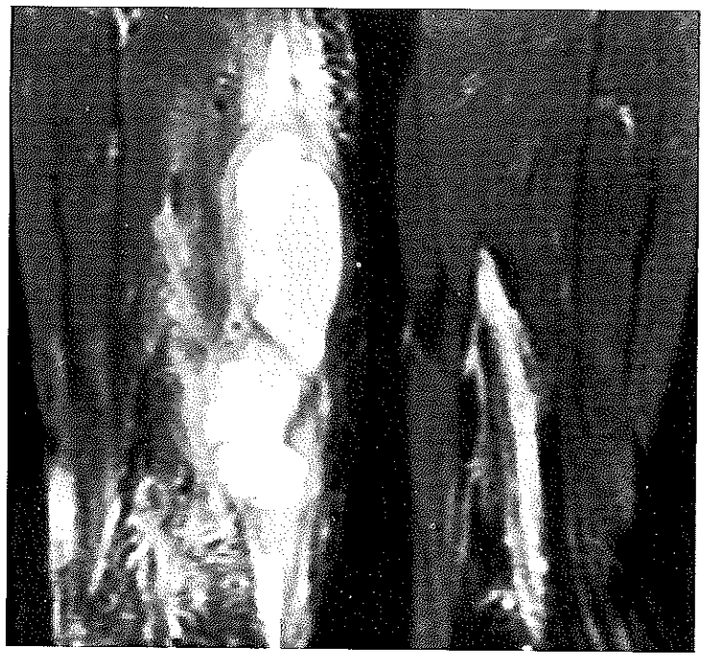

FIGURE 18C

REFERENCES

1. **Kahn, D. S. and Pritzker, K. P. H.,** The pathophysiology of bone infection, *Clin. Orthop.,* 96, 12, 1973.
2. **Hobo, T.,** Zur Pathogenese der Akuten Hematogenen Oteomyelitis, mit Berucksichtigung der Vital Farbungslehre, *Acta Sch. Med. Univ. Imp. Kioto.,* 4, 1, 1922.
3. **Trueta, J.,** The three types of acute hematogenous osteomyelitis, *J. Bone Jt. Surg.,* 41B, 671, 1959.
4. **Capitanio, M. A. and Kirkpatrick, J. A.,** Early roentgen observations in acute osteomyelitis, *Am. J. Roentgenol.,* 130, 488, 1970.
5. **Waldvogel, F. A., Medoff, G., and Swartz, M. N.,** Osteomyelitis: a review of clinical features, therapeutic considerations and unusual aspects (first of three parts), *N. Engl. J. Med.,* 282, 198, 1970.
6. **Bar-Ziv, J., Barki, Y., Maroko, A., and Mares, A. J.,** Rib osteomyelitis in children: early radiologic and ultrasonic findings, *Pediatr. Radiol.,* 15, 315, 1985.
7. **Resnick, D. and Niwayama, G.,** Osteomyelitis, septic arthritis, and soft-tissue infection: the mechanisms and situations, in *Diagnosis of Bone and Joint Disorders,* 2nd ed., W.B. Saunders, Philadelphia, 1988, 2546.
8. **Mettler, F. A. and Guiberteau, M. J.,** Skeletal system, in *Essentials of Nuclear Medicine Imaging,* W.B. Saunders, Philadelphia, 1991, 209.
9. **Maurer, A. H., Chen, D. C. P., Camargo, E. E., Wong, D. F., Wagner, H. N., and Alderson, P. O.,** Utility of three-phase skeletal scintigraphy in suspected osteomyelitis: concise communication, *J. Nucl. Med.,* 22, 941, 1981.
10. **Seldin, D. W., Heiken, J. P., Feldman, F., and Alderson, P. O.,** Effect of soft-tissue pathology on detection of pedal osteomyelitis in diabetics, *J. Nucl. Med.,* 26, 988, 1985.
11. **Alazraki, N., Dries, D., Datz, F., Lawrence, P., Greenberg, E., and Taylor, A., Jr.,** Value of a 24-hour image (four-phase bone scan) in assessing osteomyelitis in patients with peripheral vascular disease, *J. Nucl. Med.,* 26, 711, 1985.
12. **Israel, O., Gips, S., Jerushalmi, J., Frenkel, A., and Front, D.,** Osteomyelitis and soft-tissue infection: differential diagnosis with 24 hour/4 hour ratio of Tc-99m MDP uptake, *Radiology,* 163, 725, 1987.
13. **Ash, J. A., and Gilday, D. L.,** The futility of bone scanning in neonatal osteomyelitis: concise communication, *J. Nucl. Med.,* 21, 417, 1980.
14. **Raptopoulos, V., Doherty, P. W., Goss, T. P., King, M. A., Johnson, K., and Gantz, N. M.,** Acute osteomyelitis: advantage of white cell scans in early detection, *Am. J. Roentgenol.,* 139, 1077, 1982.
15. **Rosenthall, L., Lisbona, R., Hernandez, M., and Hadjipavlon, A.,** 99m Tc-PP and 67-Ga imaging following insertion of orthopedic devices, *Radiology,* 133, 717, 1979.
16. **Schauwecker, D. S., Park, H. M., Mock, B. H., Burt, R. W., Kernick, C. B., Ruoff, A. C., Sinn, H. J., and Wellman, H. N.,** Evaluation of complicating osteomyelitis with Tc-99m MDP, In-111 granulocytes and Ga-67 citrate, *J. Nucl. Med.,* 25, 849, 1984.
17. **Tumeh, S. S., Aliabadi, P., Weissman, B. N., and McNeil, B. J.,** Chronic osteomyelitis: bone and gallium scan patterns associated with active disease, *Radiology,* 158, 685, 1986.
18. **Sorsdahl, O. A., Goodhart, G. L., Williams, H. T., Hanna, L. J., and Rodriquez, J.,** Quantitative bone gallium scintigraphy in osteomyelitis, *Skeletal Radiol.,* 22, 239, 1993.
19. **Datz, F. L. and Thorne, D. A.,** Effect of antibiotic therapy on the sensitivity of indium-111-labeled leukocyte scans, *J. Nucl. Med.,* 27, 1849, 1986.
20. **Schauwecker, D. S.,** Osteomyelitis: diagnosis with In-111-labeled leukocytes, *Radiology,* 171, 141, 1989.
21. **Kim, E. E., Pjura, G. A., Lowry, P. A., Gobuty, A. H., and Traina, J. F.,** Osteomyelitis complicating fracture: pitfalls of 111-In leukocyte scintigraphy, *Am. J. Roentgenol.,* 148, 927, 1987.

22. **Palestro, C. J., Kim, K. K., Swyer, A. J., Capozzi, J. D., Solomon, R. W., and Goldsmith, S. J.,** Total-hip arthroplasty: periprosthetic Indium-111-labeled leukocyte activity and complementary Technetium-99m-sulfur colloid imaging in suspected infection, *J. Nucl. Med.*, 31, 1950, 1990.
23. **Fischman, A., Rubin, R. H., Khaw, B. A., Callahan, R. J., Wilkinson, R., Keech, F., Nedelman, M., Dragotakes, S., Kramer, P. B., LaMuraglia, G. M., Lind, S., and Strauss, H. W.,** Detection of acute inflammation with 111-In-labeled nonspecific polyclonal IgG, *Semin. Nucl. Med.*, 18, 335, 1988.
24. **Lantto, E. H., Lantto, T. J., and Vorne, M.,** Fast diagnosis of abdominal infections and inflammations with technetium-99m-HMPAO labeled leukocytes, *J. Nucl. Med.*, 32, 2029, 1991.
25. **McAfee, J. G., Gagne, G., Subramanian, G., and Schneider, R. F.,** The localization of Indium-111-leukocytes, gallium-67-polyclonal IgG and other radioactive agents in acute focal inflammatory lesions, *J. Nucl. Med.*, 32, 2126, 1991.
26. **Berquest, T. H., Brown, M. L., Fitzgerald, R. H., and May, G. R.,** Magnetic resonance imaging: application in musculoskeletal infection, *Magnet. Reson. Imag.*, 3, 219, 1985.
27. **Kuhn, J. P. and Berger, P. E.,** Computed tomographic diagnosis of osteomyelitis, *Radiology*, 130, 503, 1979.
28. **Hermann, G. and Rose, J. S.,** Computed tomography in bone and soft tissue pathology of the extremities, *J. Comput. Assist. Tomogr.*, 3, 58, 1979.
29. **Wing, V. W., Jeffrey, R. B., Federle, M. P., Helms, C. A., and Trafton, P.,** Chronic osteomyelitis examined by CT, *Radiology*, 154, 171, 1985.
30. **Ram, P. C., Martinez, S., Korobkin, M., Beriman, R. S., Gallis, H. R., and Harrelson, J. M.,** CT detection of intraosseous gas: a new sign of osteomyelitis, *Am. J. Roentgenol.*, 137, 721, 1981.
31. **Seltzer, S. E.,** Value of computed tomography in planning medical and surgical treatment of chronic osteomyelitis, *J. Comput. Assist. Tomogr.*, 8 482, 1984.
32. **Modic, M. T., Feiglin, D. H., Piraino, D. W., Boumphrey, F., Weinstein, M. A., Duchesneau, P. M., and Rehm, S.,** Vertebral osteomyelitis: assessment using MR, *Radiology*, 157, 157, 1985.
33. **Unger, E., Moldofsky, P., Gatenby, R., Hartz, W., and Broder, G.,** Diagnosis of osteomyelitis by MR imaging, *Am. J. Roentgenol.*, 150, 605, 1988.
34. **Tang, J. S. H., Gold, R. H., Bassett, L. W., and Seeger, L. L.,** Musculoskeletal infection of the extremities: evaluation with MR imaging, *Radiology*, 166, 205, 1988.
35. **Mason, M. D., Zlatkin, M. B., Esterhai, J. L., Dalinka, M. K., Velchik, M. G., and Kressel, H. Y.,** Chronic complicated osteomyelitis of the lower extremity: evaluation with MR imaging, *Radiology*, 173, 355, 1989.
36. **Wang, A., Greenfield, L., Chiu, L., Chambers, R., Stewart, C., Hung, G., Diaz, F., and Ellis, T.,** MRI and diabetic foot infections, *Magnet. Resonan. Imag.*, 8, 805, 1990.
37. **Erdman, W. A., Tamburro, F., Jayson, H. T., Weatherall, P. T., Ferry, K. B., and Peshock, R. M.,** Osteomyelitis: characteristics and pitfalls of diagnosis with MR imaging, *Radiology*, 180, 533, 1991.
38. **Seabold, J. E., Flickinger, F. W., Kao, S. C. S., Gleason, T. J., Kahn, D., Nepola, J. V., and Marsh, J. L.,** Indium-111-leukocyte/technetium-99m-MDP bone and magnetic resonance imaging: difficulty of diagnosing osteomyelitis in patients with neuropathic osteoarthropathy, *J. Nucl. Med.*, 31, 549, 1990.
39. **Bamberger, D. M., Daus, G. P., and Gerding, D. N.,** Osteomyelitis in the feet of diabetic patients: long-term results, prognostic factors, and the role of antimicrobial and surgical therapy, *Am. J. Med.*, 83, 653, 1987.
40. **Newman, L. G., Waller, J., Palestro, C. J., Schwartz, M., Klein, M. J., Hermann, G., Harrington, E., Harrington, M., Roman, S. H., and Stagnaro-Green, A.,** Unsuspected

osteomyelitis in diabetic foot ulcers: diagnosis and monitoring by leukocyte scanning with indium In 111 oxyquinoline, *JAMA*, 266, 1246, 1991.

41. **Caprioli, R., Testa, J., Cournoyer, R. W., Jr., and Esposito, F. J.,** Prompt diagnosis of suspected osteomyelitis by utilizing percutaneous bone culture, *J. Foot Surg.*, 25, 263, 1986.
42. **Sapico, F. L., Witte, J. L., Canawati, H. N., Montgomerie, J. Z., and Bessman, A. N.,** The infected foot of the diabetic patient: quantitative microbiology and analysis of clinical features, *Rev. Infect. Dis.*, 6(Suppl. 1), S171, 1984.
43. **Perry, C. R., Pearson, R. L., and Miller, G. A.,** Accuracy of cultures of material from swabbing of the superficial aspect of the wound and needle biopsy in the preoperative assessment of osteomyelitis, *J. Bone Jt. Surg.*, 73A, 745, 1991.
44. **Weinstein, D., Wang, A., Chambers, R., Stewart, C. A., and Motz, H. A.,** Evaluation of MRI in the diagnosis of osteomyelitis in diabetic foot infection, *Foot Ankle*, 14, 18, 1993.
45. **Park, H. M., Wheat, J., Siddiqui, A. R., Burt, R. W., Robb, J. A., Ransburg, R. C., and Kernek, C. B.,** Scintigraphic evaluation of diabetic osteomyelitis: concise communication, *J. Nucl. Med.*, 23, 569, 1982.
46. **Larcos, G., Brown, M. L., and Sutton, R. T.,** Diagnosis of osteomyelitis of the foot in diabetic patients: value of ^{111}In-leukocyte scintigraphy, *Am. J. Roentgenol.*, 157, 527, 1991.
47. **Keenan, A. M.,** Diagnosis of pedal osteomyelitis in diabetic patients using current scintigraphic techniques, *Arch. Intern. Med.*, 149, 2262, 1989.
48. **Maurer, A. H., Millmond, S. H., Knight, L. C., Mesgardeh, M., Siegel, J. A., Shuman, C. R., Adler, L. P., Greene, G. S., and Malmud, L. S.,** Infection in diabetic osteoarthropathy: use of indium-labeled leukocytes for diagnosis, *Radiology*, 161, 221, 1986.
49. **Schauwecker, D. S., Park, H. M., Burt, R. W., Mock, B. H., and Wellman, H. N.,** Combined bone scintigraphy and indium-111 leukocyte scans in neuropathic foot disease, *J. Nucl. Med.*, 29, 1651, 1988.
50. **Unger, E., Moldofsky, P., Gatenby, R., Hartz, W., and Broder, G.,** Diagnosis of osteomyelitis by MR imaging, *Am. J. Roentgenol.*, 150, 605, 1988.
51. **Yuh, W. T. C., Corson, J. D., Baraniewski, H. M., Rezai, K., Shamma, A. R., Kathol, M. H., Sato, Y., El-Khoury, G. Y., Hawes, D. R., Platz, C. E., Cooper, R. R., and Corry, R. J.,** Osteomyelitis of the foot in diabetic patients: evaluation with plain film, 99m-MDP bone scintigraphy, and MR imaging, *Am. J. Roentgenol.*, 152, 795, 1989.
52. **Wang, A., Weinstein, D., Greenfield, L., Chiu, L., Chambers, R., Stewart, C., Hung, G., Diaz, F., and Ellis, T.,** MRI and diabetic foot infections, *Magnet. Resonan. Imag.*, 8, 805, 1990.
53. **Sugarman, B., Hawes, S., Musher, D. M., Klima, A., Young, E. J., and Pircher, F.,** Osteomyelitis beneath pressure sores, *Arch. Intern. Med.*, 143, 683, 1983.
54. **Resnick, D. and Niwayama, G.,** Osteomyelitis, septic arthritis, and soft-tissue infection: the mechanisms and situations, in *Diagnosis of Bone and Joint Disorders*, 2nd ed., W.B. Saunders, Philadelphia, 1988, 2540.
55. **Anthony, J. P. and Mathes, S. J.,** Update on chronic osteomyelitis, *Clin. Plastic Surg.*, 18, 515, 1991.
56. **Meadows, S. E., Zuckerman, J. D., and Koval, K. J.,** Posttraumatic tibial osteomyelitis: diagnosis, classification, and treatment, *Hospital for Joint Disease Bulletin*, 52, 11, 1993.
57. **Tumeh, S. S., Aliabadi, P., Weissman, B. N., and McNeil, B. J.,** Disease activity in osteomyelitis: role of radiography, *Radiology*, 165, 781, 1987.
58. **Merkel, K. D., Brown, M. L., Dewanjee, M. K., and Fitzgerald, R. H., Jr.,** Comparison of indium-labelled-leukocyte imaging with sequential technetium-gallium scanning in the diagnosis of low-grade musculoskeletal sepsis, *J. Bone Jt. Surg.*, 67A, 465, 1985.
59. **Tumeh, S. S., Aliabadi, P., Weissman, B. N., and McNeil, B. J.,** Chronic osteomyelitis: bone and gallium scan patterns associated with active disease, *Radiology*, 158, 685, 1986.

60. **Sfakianakis, G. N., Al-Sheikh, W., Heal, A., Rodman, G., Zeppa, R., and Serfini, A.,** Comparisons of scintigraphy with In-111 leukocytes and Ga-67 in the diagnosis of occult sepsis, *J. Nucl. Med.,* 23, 618, 1982.
61. **Datz, F. L. and Thorne, D. A.,** Effect of chronicity of infection on the sensitivity of the In-111-labeled leukocyte scan, *Am. J. Roentgenol.,* 147, 809, 1986.
62. **Quinn, S. F., Murray, W., Clark, R. A., and Cochran, C.,** MR imaging of chronic osteomyelitis, *J. Comput. Assist. Tomogr.,* 12, 113, 1988.
63. **Bjorksten, B. and Boquist, L.,** Histopathologic aspects of chronic recurrent multifocal osteomyelitis, *J. Bone Jt. Surg.,* 62B, 376, 1980.
64. **Murray, S. D. and Kehl, D. K.,** Chronic recurrent multifocal osteomyelitis, *J. Bone Jt. Surg.,* 71A, 105, 1984.
65. **Brown, T. and Wilkinson, R. H.,** Chronic recurrent multifocal osteomyelitis, *Radiology,* 166, 493, 1988.
66. **Bjorksten, B., Gustavson, K. H., Eriksson, B., Lindholm, A., and Nordstrom, S.,** Chronic recurrent multifocal osteomyelitis and pustulosis palmoplantaris, *J. Pediatr.,* 93, 227, 1978.
67. **Rosenbaum, D. M. and Blumhagen, J. D.,** Acute epiphyseal osteomyelitis in children, *Radiology,* 156, 89, 1985.
68. **Singson, R. D., Berdon, W. E., Feldman, F., Denton, J. R., Abramson, S., and Baker, D. H.,** "Missing" femoral condyle: an unusual sequela to neonatal osteomyelitis and septic arthritis, *Radiology,* 161, 359, 1986.
69. **Nade, S.,** Acute haematogenous osteomyelitis in infancy and childhood, *J. Bone Jt. Surg.,* 65B, 109, 1983.
70. **Dagan, R.,** Management of acute hematogenous osteomyelitis and septic arthritis in the pediatric patient, *Pediatr. Infect. Dis. J.,* 12, 88, 1993.
71. **Fleisher, G. R., Paradise, J. E., Plotkin, S. A., and Borden, S., IV.,** Falsely normal radionuclide scans for osteomyelitis, *Am. J. Dis. Child.,* 134, 499, 1980.
72. **Howie, D. W., Savage, J. P., Wilson, T. G., and Paterson, D.,** The technetium phosphate bone scan in the diagnosis of osteomyelitis in childhood, *J. Bone Jt. Surg.,* 65A, 431, 1983.
73. **Sullivan, D. C., Rosenfield, N. S., Ogden, J., and Gottschalk, A.,** Problems in the scintigraphic detection of osteomyelitis in children, *Radiology,* 135, 731, 1980.
74. **Lewin, J. S., Rosenfield, N. S., Hoffer, P. B., and Downing, D.,** Acute osteomyelitis in children: combined Tc-99m and Ga-67 imaging, *Radiology,* 158, 795, 1986.
75. **Hitchon, P. W., Osenbach, R. K., Yoj, W. T. C., and Menezes, A. H.,** Spinal infections, *Clinical Neurosurg.,* 38, 373, 1992.
76. **Antunes, J.,** Infections of the spine, *Acta. Neurochir. (Wien),* 116, 79, 1992.
77. **McHenry, M. C., Rehm, S. J., Krajewski, L. P., Duchesneau, P. M., Levin, H. S., and Steinmuller, D. R.,** Vertebral osteomyelitis and aortic lesions: case report and review, *Rev. Infect. Dis.,* 13, 1184, 1991.
78. **Post, M. J. D., Bowen, B. C., and Sze, G.,** Magnetic resonance imaging of spinal infection, *Imag. Rheum. Dis.,* 17, 773, 1991.
79. **Numaguchi, Y., Rigamonti, D., Rothman, M. I., Sato, S., Mihara, F., and Sadato, N.,** Spinal epidural abscess: evaluation with gadolinium-enhanced MR imaging, *Radiographics,* 13, 545, 1993.
80. **Schlaeffer, F., Mikolich, D. J., and Mates, S. M.,** Technetium Tc 99m diphosphonate bone scan: false-normal findings in elderly patients with hematogenous vertebral osteomyelitis, *Arch. Intern. Med.,* 147, 2024, 1987.
81. **Crim, J. R., Seeger, L. L., Yao, L., Chandnani, V., and Eckardt, J. J.,** Diagnosis of soft-tissue masses with MR imaging: can benign masses be differentiated from malignant ones?, *Radiology,* 185, 581, 1992.